

X-641-67-274

29A NASA-TM-X-55814-6

3 THE IRON METEORITES,
THEIR THERMAL HISTORY,
AND PARENT BODIES 6

6 JOSEPH I. GOLDSTEIN
JAMES M. SHORT 9

N67-29991

FACILITY FORM 602

(ACCESSION NUMBER)

1085RS-1A

(PAGES)

TMX-5581K

(NASA CR OR TMX OR AD NUMBER)

(THRU)

1
(CODE)

30
(CATEGORY)

9 JUNE 1967/0



1. NASA

— GODDARD SPACE FLIGHT CENTER —

GREENBELT, MARYLAND 3

THE IRON METEORITES, THEIR THERMAL HISTORY,
AND PARENT BODIES

Joseph I. Goldstein
Geochemistry Laboratory
Laboratory for Theoretical Studies
Goddard Space Flight Center - NASA
Greenbelt, Maryland, 20771

and

James M. Short*
Space Sciences Division
Ames Research Center - NASA
Moffett Field, California, 94035

* Present Location:

Branch of Analytical Chemistry
U. S. Geological Survey
Menlo Park, California

The Iron Meteorites, Their Thermal History and Parent Bodies

J. I. Goldstein and J. M. Short

ABSTRACT

Cooling rates are determined for the formation of the Widmanstätten pattern in 193 iron meteorites in order to obtain information on the number and possible types of parent meteorite bodies. About two thirds of the meteorites cooled between 1 and 10°C/m.y. although the total variation in cooling rates is 0.4 to 500°C per million years. These variations indicate that the iron meteorites formed in more than one parent body, the Widmanstätten pattern formed at low pressures, and the maximum sized parent body was about 300 km in radius if the irons formed in its core.

Evidence is presented to show that meteorites, in the Ga-Ge groups are genetically related. Characteristic plessite structures were observed for each of these groups. The cooling rate variations in both Ga-Ge groups I and IIIb are small (2-3°C/m.y. and 1-2°C/m.y., respectively) and independent of chemical composition. These meteorites probably formed in the cores of parent bodies about 200 km in radius. The cooling rate variations in both groups IIIa and IVa are large (1.5-10°C/m.y. and 7-90°C/m.y., respectively) and vary with the Ni content, decreasing as the Ni content increases. These meteorites probably formed in isolated regions spread throughout parent bodies 150-200 km in radius. These regions consisted of molten metal at the time of formation.

The Iron Meteorites, Their Thermal History and Parent Bodies

J. I. Goldstein and J. M. Short

INTRODUCTION

Meteorites are generally assumed to be fragments of preexisting "parent bodies." One of the central problems in meteoritics has been to determine the number, location, and structure of these meteorite parent bodies. Using the vast amount of physical and chemical data which have been measured, investigators have found that large numbers of meteorites are related and may be considered members of discrete groups. These groups can be defined when the member meteorites have measured chemical or physical properties which cluster. This clustering suggests that the meteorites have been genetically related within a parent body. However, the sensitivity of each measured property or parameter to the original environment of the meteorite within the parent body varies. Some meteorites can be grouped by one property but not by others. The best way to remove such ambiguities is to correlate several sensitive parameters, some of which are capable of direct physical interpretation. The cooling rate is an ideal physical property for such use, since its value is highly dependent on the composition and heat source as well as on the location of the meteorite within the parent body.

The cooling rate or thermal history of meteorites can be revealed by studying the structures developed in the metallic phases. In particular, the iron meteorites are most easily investigated since a Widmanstätten pattern forms by the precipitation of kamacite from the parent taenite phase. In the last few years our understanding of the development of the Widmanstätten pattern has increased greatly mainly through the use of the electron probe (Short and Anderson, 1965, Reed, 1965) and computer programs which simulate its growth (Wood, 1964, Goldstein and Ogilvie, 1965, Goldstein and Short, 1967). In fact we are now able to determine cooling rates for iron meteorites, which are a direct measure of their thermal history.

Until now, only a few cooling rates have been determined. Using modified and faster methods (Short and Goldstein, 1967) we have been able to determine the cooling rates of the Widmanstätten structure in 193 iron meteorites, representing over one third of the known irons. These data as well as correlations with other properties provide the basis for a discussion of the possible types of parent bodies in which these meteorites formed.

Methods for Determining Cooling Rates

A. Method of Analysis

Kamacite (α) and taenite (γ) in iron meteorites are essentially Fe-Ni solid solutions containing, respectively, 5-7.5% and 15-50 wt % Ni. As the meteorite cooled through the temperature range 700°-300°C, α phase nucleated in γ phase and grew by solid-state diffusion (Figure 1). The α plates form the unique pattern called the Widmanstätten structure. At lower temperatures decreasing diffusion rates caused compositional zoning next to the borders of taenite and kamacite. These can be easily measured with an electron microprobe (Short and Anderson, 1965; Reed, 1965).

The complex method which we have developed (Goldstein and Short, 1967) for determining the cooling rate of the Widmanstätten structures uses the known phase equilibria and diffusion coefficients in the Fe-Ni system. It also takes into account all the following factors which influence the formation at the Widmanstätten structure: a) the bulk nickel content of the meteorite; b) undercooling below the equilibrium α - precipitation temperature; c) impingement of neighboring kamacite plates; d) the cooling rate of the meteorite; e) pressure. Goldstein and Ogilvie (1965) have shown that the pressure at the locations of the iron meteorites within the parent bodies was apparently not sufficient (< 10 kb) to influence the growth of kamacite. The other factors (a-d) determine the ultimate kamacite bandwidth and the shape of the retained diffusion gradients in both taenite and kamacite. The observed kamacite bandwidths and diffusion gradients match in exact detail those calculated for a unique cooling rate.

Recently Short and Goldstein (1967) have developed two rapid methods for obtaining the cooling rate of meteorites with a Widmanstätten pattern. These methods are based on the precise method and yield cooling rates within $\pm 50\%$ of those obtained by the more complicated computer calculation of Goldstein and Short, 1967. The basis for the one of the rapid methods lies in assuming values for undercooling and impingement. The cooling rate can then be obtained by a simple measurement of bulk nickel content and kamacite plate thickness. The assumptions underlying the method will now be discussed in more detail.

1. Undercooling - When a meteorite is classified according to its structure, the kamacite bandwidth is used. The kamacite bands are usually the largest sized platelets in the meteorite and presumably were the first kamacite areas to form as the meteorite cooled into the $\alpha + \gamma$ field of the Fe-Ni phase diagram (Fig. 1). In our study of the cooling rate of 27 meteorites using the complex computer calculation method, we found that undercooling of $110^{\circ}\text{C} \pm 15^{\circ}\text{C}$ occurred in 90% of the kamacite bands studied. No significant differences in undercooling were found between different groups of meteorites or between meteorites with different cooling rates or nickel contents. Therefore undercooling of 110°C below the $\gamma / (\alpha + \gamma)$ boundary in the Fe-Ni phase diagram was assumed for the kamacite bands which define the Widmanstätten pattern.

2. Impingement - The effect of impingement is related to the distance between nucleation sites for the Widmanstätten pattern, since this distance determines the maximum size that the kamacite phase can attain. The result of impingement is to increase the central nickel content of the taenite above the original composition of the meteorite. It may also restrict the amount of kamacite growth. This effect is illustrated in Figure 2. The resultant Ni

concentration gradients are calculated for a kamacite plates nucleating 110°C below the $\gamma / (\alpha + \gamma)$ boundary in a meteorite of 10 wt. % Ni, cooling at a rate of 1°C/m.y. The calculation was performed for several different values of X_0 , the distance between nucleation sites for the Widmanstätten pattern. The kamacite band width obtained when the distance between nucleation sites X_0 is effectively infinite is W_{∞} . Two types of impingement can occur: Type I, $X_0 \geq W_{\infty}$. The effect of impingement is only to increase the central Ni content of taenite. This increase is usually to a level of no more than 25-30 wt. % Ni. The resultant kamacite band width is little affected (see Figure 2). This is reasonable since 80% of the growth of the Widmanstätten pattern occurs in the first 50°C of cooling after nucleation during which diffusion rates are fastest but impingement is insignificant. In this case, one can assume that the effect of impingement is negligible. Type II, $X_0 < W_{\infty}$. The effect of impingement is not only to increase the central Ni content and but also to decrease the kamacite band width, (see Figure 2). The Ni content in taenite is usually greater than 30 wt % Ni. When Type II impingement occurs, one cannot assume that the effect of impingement is negligible. Calculations for meteorites with 7, 8, 12.5, 17 and 25 wt % Ni show the same Type I, Type II impingement effects.

Whether Type II impingement occurs can usually be determined by metallographic inspection of the taenite area between the impinging bands. If plessite in the form of kamacite plates or martensitic α_2 has formed, the Ni content is less than 25-30 wt. %, and X_0 is greater than W_{∞} . If plessite is not present, the Ni content is greater than 30 wt. % and significant impingement has occurred. In this case the rapid cooling rate method is not applicable.

The effect of impingement is negligible in meteorites with high Ni contents and fast cooling rates since nucleation occurs at relatively low temperatures and little time is available for the growth process. Therefore in ataxites and many octahedrites of fine structure the diffusion gradients in taenite do not extend to the center of the phase. Impingement becomes more prevalent for meteorites as the Ni content and cooling rate decreases. However, it is only for meteorites with low Ni contents, usually ≤ 8 wt. % Ni, and slow cooling rates $\leq 2^\circ\text{C/m.y.}$ that impingement of type II may be important.

Assuming 1) undercooling of 110°C below the $\gamma / (\alpha + \gamma)$ boundary in the Fe-Ni phase diagram and 2) no impingement, computer calculations of the kamacite plate thickness (W_∞) were made as a function of cooling rate and bulk Ni content (Figure 3). Under these limiting conditions a cooling rate can be determined rapidly by using the kamacite band width and the bulk Ni content.

The calculation of kamacite growth for meteorites with less than 6.85 wt. % Ni was not performed because the form of the $\alpha / (\alpha + \gamma)$ phase boundary below 500°C which has not been determined experimentally has a large effect on the growth process. The ataxites and many fine octahedrites have such steep Ni gradients in taenite that these gradients cannot be measured with the electron probe and therefore are not subject to the precise cooling rate method. This rapid method, however, allows us for the first time to obtain cooling rates for these meteorites since only the band width and Ni content are needed.

B. Selection and Sample Preparation of Meteorites.

The number of individual octahedrites and ataxites catalogued totals over 400. Recent chemical analyses of iron meteorites are available for less than 200 of these meteorites. Samples of 193 meteorites were obtained for band width measurement. Satisfactory samples were those which contained at least

10-20 kamacite bands which defined the Widmanstätten pattern and had at least one side cut perpendicular to the polished surface. The size of the sample might vary from 5 grams for an ataxite to several hundred grams for a coarse octahedrite.

All these meteorites were polished by standard metallographic techniques. At least 10 bands were measured on each meteorite, either on photomicrographs or microscopically with a calibrated eyepiece micrometer. The kamacite bands selected were major bands which establish the gross Widmanstätten structure. They overlap other smaller kamacite bands which develop later in the cooling process. Inclusions such as schreibersite or cohenite which serve to increase the apparent bandwidth were avoided. Also kamacite plates were chosen which were not bordered by a taenite band showing severe (Type II) impingement effects. Bandwidths cannot be suitably measured without polishing the sample and examining it with the above criteria in mind. The band system of the Widmanstätten pattern chosen for measurement intersects the section surface at a steep angle. The measured kamacite bandwidths were related to plate thickness by determining the dip-angle of the plates by angle measurements on the top surface and a second perpendicular surface (c.f. Nevin, 1949). In several ataxites and transitional meteorites the orientation of the kamacite plates could not be determined because the plates were too small. In this case the resultant cooling rates may be in error by as much as $\pm 100\%$.

Even when kamacite bands were selected by the above criteria differences between the measured bandwidths were found. These differences are probably caused by varying nucleation temperatures. Bandwidth distributions for two meteorites, Edmonton and Mt. Edith, are shown in Figure 4. Edmonton is a

fine octahedrite with long overlapping, well defined kamacite bands. Mt. Edith is a medium octahedrite with short overlapping kamacite bands and a Widmanstatten pattern often broken by inclusions. Edmonton represents the type of meteorite whose bandwidth is easily determined; Mt. Edith, represents the type of meteorite, whose bandwidth is difficult to determine.

The bandwidth distributions for both meteorites (Figure 4) are roughly Gaussian. The maximum band width is established by the first kamacite bands to form. A minimum bandwidth is also measured. Bands below this minimum no longer cross other kamacite plates and do not establish the major texture of the meteorite. The "kamacite bandwidth" as measured in this study is the average or mean of the bandwidth distribution. A $\pm 10\%$ deviation from the mean kamacite bandwidth includes 70% of the bands in the best case (Edmonton) and 50% of the bands in the worst case (Mt. Edith). A $\pm 20\%$ deviation from the kamacite bandwidth includes 95% and 85% of the bands respectively. Therefore a deviation of $\pm 10\%$ represents about one standard deviation and $\pm 20\%$ represents about two standard deviations for an infinite sample. The measurement of the minimum 10 bands per meteorite increases these limits by about 25% (Proschan, 1953). For almost all the samples studied we were able to measure the kamacite bandwidth to $\pm 10\%$ with a high degree of confidence. This deviation represents an error in the cooling rate of no more than $\pm 25\%$.

Results

Cooling Rate Data

Kamacite plate thicknesses were measured and cooling rates determined for 193 octahedrites, transitional octahedrites and ataxites with Ni contents

from 6.85 wt. % Ni to 30 wt. % Ni. The measured band widths, the Ni contents and the measured cooling rates are listed in Table 1. When kamacite plate thicknesses were measured by both authors, two values were reported. Kamacite plate thicknesses measured by Lovering (1956) are also included and un-oriented kamacite bands are noted by the symbol ~ before the value of the bandwidth. When non-oriented kamacite bands were used or when the Ni contents or kamacite band widths have a range of values, only approximate cooling rates are given.

Band Width Distribution

The distribution of band widths for all the irons measured is shown in the form of a histogram in figure 5. As discussed previously, iron meteorites with Ni contents below 6.85 wt. % Ni were not studied. Therefore the coarsest octahedrites and hexahedrites are not represented in our distribution plots. In other respects, the histogram is quite similar to that of Lovering, et. al (1957). Most of the meteorites have band widths between 0.5 and 1.5 mm and no sharp breaks appear in the band width distribution. The peak in the distribution found at 0.3 mm corresponds to a large number of meteorites with fine structure and low Ni contents. To place meteorites in their appropriate textural groups, the classification system according to Buchwald and Munck (1965) in a slightly modified form was used (Table 2).

The scale was chosen so that each step represents a doubling in the band width. For band widths less than 0.25 mm, iron meteorites have three distinctly different types of texture: Off, the kamacite bands which determine the Widmanstatten pattern < 0.25 mm in width; D, ataxite, individual kamacite bands

forming a micro-Widmanstätten pattern in which only a few bands intersect; Off-D, transitional between both types. The meteorite structures are also listed in Table 1. Since the kamacite bands vary in width by about ± 10 to 20%, it is difficult to distinguish in many cases whether a meteorite belongs in one textural class or another.

Cooling Rates

The cooling rates given in Table 1 are plotted in a histogram in Figure 6. The cooling rates vary over three orders of magnitude, from 0.4° to $> 500^\circ\text{C/m.y.}$ This large variation indicates that all of these meteorites could not have cooled in the same area of one parent body. The cooling rate histogram is asymmetric with an abrupt cut-off in cooling rate at 0.4°C/m.y. The three meteorites with the lowest cooling rates, Brenham, Glorieta and Butler, are unusual. Brenham and Glorieta are pallasites with large metal areas of octahedral structure and Butler has a texture transitional between octahedrites and ataxites with an unusually high Ge content of 2000 ppm (Wasson, 1966). The cooling rate distribution does not have any sharp breaks. However, a small peak between $50\text{--}100^\circ\text{C/m.y.}$ is apparent along with the main peak between $1.5\text{--}3^\circ\text{C/m.y.}$ About two thirds of the meteorites cooled between 1 and 10°C/m.y.

In Figure 6 separate cooling rate histograms are shown for meteorites in the various textural classifications. The cooling rate varies by at least a factor of 10 in each class (the measurement precision is $\pm 50\%$) and in general the average cooling rate of each class increases with the fineness of the Widmanstätten pattern. The ataxites as a group cooled faster than any of the iron

meteorites. A summary of the cooling rate and Ni variations in each textural class is given in Table 3. In each class the lowest Ni content corresponds to the fastest cooling rate. Also the dispersion in Ni contents and cooling rates becomes larger in the meteorites with very fine Widmanstätten patterns. Not enough members of the Ogg class were measured to obtain any reliable variations. In our sample only meteorites with band widths of less than 0.5mm cooled faster than $25^{\circ}/\text{m.y.}$ Only the transitional and ataxite irons had members which cooled faster than $100^{\circ}\text{C}/\text{m.y.}$

Cooling Rates in the Gallium-Germanium Groups

The Ga and Ge contents of most iron meteorites fall into sharply defined clusters, instead of forming a continuous distribution (Goldberg, et al. 1951, Lovering et al. 1957). This fact has served as the basis for placing meteorites into one of several Ga-Ge groups. It has also been suggested that the Ga-Ge groups have genetic significance and that member meteorites formed in the same parent body (Anders, 1964). Wasson (1967a), with improved chemical techniques, has found very closely correlated Ga-Ge-Ni-structural groups. Five groups have been resolved to date. The Ni and Ge variations within each group are listed in Table 4. In Groups IIIa, IVa and IVb the Ge is directly correlated with the Ni, but in Groups IIIb and IVa an inverse correlation is observed. Wasson (1967a, c) has suggested that each of these groups comes from a separate meteorite parent body. Presumably if the meteorites in each parent body formed in a core, they would have the same cooling rate. The individual Ni, Ge and P contents as well as the cooling rate for each of the meteorites in the Ga-Ge groups are listed in Tables 5 to 9. The Ge values were determined by Wasson

(1967a, b, c) and the P contents by Moore and Lewis (1967). The meteorites within each group are listed by increasing Ni content. Large variations in cooling rate were observed for Groups IIIa, IVa and IVb (Table 4). It should be noted that, as a result of using the rapid method to determine cooling rates, a 100% variation in cooling rate within a single group might be expected. Larger variations cannot be ascribed to the method.

The variations can be more fully understood by reference to the cooling rate histograms in Figure 6 where the various Ga-Ge groups are outlined. In Figure 7 we have plotted the variation of cooling rate and Ni content for the member meteorites of the 5 Ga-Ge groups. The number of meteorites represent about half of our total sample. The scatter within each group is small. Boundaries can easily be drawn around the meteorites in each group.

The cooling rate variation in both Groups I and IIIb is small and is independent of chemical composition (Ni, Ge, etc.). Such a small variation in cooling rate ($< \pm 50\%$) suggests that these meteorites may be genetically related. However, meteorites in Groups IIIa and IVa have large variations in cooling rate. The cooling rates and Ni contents correlate strongly, decreasing as the Ni content increases. It is hard to understand how these meteorites can represent the core or a single area in a parent meteorite body. Group IVb has a variation in cooling rate of a factor of 10. However, since the kamacite bands in these ataxites were not oriented, errors in the cooling rate of more than $\pm 100\%$ may be present. Therefore, the cooling rate variation and its correlation with Ni content cannot be accurately established.

Textural Relationships (Plessite)

Textural relations, particularly in the plessite, are also found for meteorites in each of the Ga-Ge groups. These relations can be used to differentiate meteorites belonging to one group from meteorites in another group and to indicate whether a new meteorite may be a possible member of the established groups.

In Group I, the meteorites show a variation in structure from coarsest octahedrites Ogg (Cranbourne band width > 2mm) to coarse-octahedrites Og (Toluca, band width = 1.1 mm). They are filled with large schreibersite-cohenite bands many of which are not oriented with the Widmanstätten pattern. These meteorites, especially those with the coarsest structure, have taenite bands which have undergone impingement with a subsequent build-up of Ni. Nevertheless, the plessite is often martensitic or, the plessitic kamacite which forms precipitates in a micro-Widmanstätten pattern much like that of the ataxites. An example of the plessite structure in Toluca is shown in Figure 8a. Group IVa meteorites have a well-defined fine Widmanstätten structure, but the plessite is all but completely transformed to kamacite. A few rounded taenite grains remain and all that defines the Widmanstätten structure is the high Ni taenite borders (Figure 8d). The Group IVb meteorites have a typical ataxite structure (Figure 8e).

Meteorites in Group IIIa have been shocked and/or reheated. The criterion for shock (> 130 kb) is the presence of ϵ iron (Heyman, et. al. 1966; Jaeger and Lipschutz, 1967). Willamette, for example, has been so badly reheated that the Widmanstätten pattern is barely visible. Most meteorites in this group have partially recrystallized kamacite and most of the plessite has been converted to

kamacite (Figure 8c). In Group IIIb the meteorites have a well-defined Widmanstätten pattern of a medium octahedrite. However, these meteorites are filled with large schreibersite bands which are not oriented with the Widmanstätten pattern and formed before the pattern developed. Many meteorites in Group IIIb show evidence of shock deformation or reheating. The plessite is mainly martensitic with a few individual resolved kamacite bands and most of the plessite has the same composition as the parent meteorite. A photomicrograph of a typical plessitic area is shown in Figure 8b. It is interesting to note that the plessite structures of the meteorites at the high Ni end of Group IIIa and the low Ni end of Group IIIb are very similar.

Discussion

Precision and Accuracy

The computer analysis on which the cooling rate values are based takes into account the variation in the measured diffusion coefficients with composition and temperature, and the variation in bulk Ni content from one iron meteorite to another (Goldstein and Short, 1967). This method has been successful in predicting the Ni gradients in both the taenite and the kamacite phase for a large number of meteorites. In the rapid method for determining cooling rates, we assumed an undercooling of 110°C below the $\gamma/(\alpha + \gamma)$ boundary in the Fe-Ni phase diagram and no impingement. The standard deviation between cooling rates for 18 meteorites, determined by the rapid method and by the computer method which considers both the undercooling and impingement as unknowns, was $\pm 50\%$. The mean percentage deviation between the two methods was only -2% . This result shows that no significant positive or negative bias is introduced by the two

simplifying assumptions. Therefore the accuracy and precision of the rapid method is dependent on the same factors as is the precise method.

The input parameters used for the computer method, which are the diffusion coefficients in the Fe-Ni system and the appropriate phase equilibria, determine the accuracy of the cooling rates. The diffusion coefficients for Fe-Ni in γ have been determined by Goldstein, Hanneman, and Ogilvie (1964) as a function of temperature, composition, and pressure above 800°C, and may be extrapolated to the temperature range in question with an estimated accuracy of better than $\pm 50\%$. Grain boundary diffusion will not contribute significantly to mass transfer between kamacite and taenite because of the extremely large crystal sizes. Recently these diffusion coefficients have been redetermined (Levasseur and Philibert, 1966) as a function of composition at 1200°C and excellent agreement was found with the previous study. The diffusion coefficients for Fe-Ni in pure Fe were also redetermined by Badia and Vignes, (1966) and are given by the equation:

$$D_{\text{Ni(Fe)}}^{\circ} = 2.8 \exp (-76,000/RT).$$

Previous relations from Goldstein et al. (1964) gave $D_{\text{Ni(Fe)}}^{\circ}$ as $3.14 \exp -(76,300/RT)$, in excellent agreement. The diffusion coefficients, were measured in Fe-Ni alloys where the C content is less than 0.01 wt%, P and S less than 0.005 wt % and Co less than 0.01 wt %. Iron meteorites typically contain (Krinov, 1960), 0.60 wt % Co, 0.17 wt % P, 0.04 wt % S, and 0.03 wt % C with small amounts of Cu, Cr, Ge, Ga, etc. Except for C the amounts of Co, P, and S are in reasonable agreement with the values of Buddhue (1946). Buddhue finds

0.2 wt % C in coarse octahedrites and lesser amounts for the fine structured octahedrites. These P, S, and C contents constitute a lower limit since analysts usually select samples free of large Schreibersite, trolite or cohenite inclusions. Wells and Mehl (1941) measured diffusion rates in Fe-Ni alloys at high temperatures and their values for 1300 and 1200°C agree very closely ($\pm 10\%$) with the more recent data. They found that C increases the Fe-Ni diffusion coefficients, by the relation;

$$D_{c_x} = D_{c_0} (1 + 2.3 \text{ wt\% C})$$

where D_{c_0} is the D value at 0% C and D_{c_x} is the D value at a carbon concentration C_x . For 0.35 wt% C, as found for rim specimens of Canyon Diablo, (Moore and Jost, 1965) $D_{c_x} = 1.81 D_{c_0}$, or D is increased by 80%. If all the C were in the γ phase, not within cohenite, the amount of growth would be increased by 30%. This would cause an error of about 30% in the cooling rate. For 0.03 wt% C, typical of the irons, the effect is less than 10%, well within the inaccuracies of the diffusion coefficient determination. Some recent C measurements (Moore and Lewis, 1967), for meteorites in Group IIIa, IIIb and IVa indicate very low C contents (Table 10). These C values are a lower limit for octahedrites with less than 8 wt % Ni (Brett, 1966). The diffusion rates in these meteorites are not affected by carbon. Meteorites containing cohenite have sufficiently high C contents (≥ 0.1 wt%) that the effect of C may be significant. Wells and Mehl (1941) also found that P and S contents up to 0.03 wt% have no effect on the diffusivities. Little work has been done on the effect of Co. However, in a preliminary paper on ternary diffusion (Sabutier and Vignes, 1966) in Fe-Ni-Co, the diffusion values of both the direct and cross coefficients are about the same indicating that Co has little effect on Fe-Ni diffusion.

The effect of trace elements is even less well known. However, the metallic elements Cr, Cu have similar bonding characteristics to Fe-Ni and at the ppm levels will not change the free energy of vacancy formation or bonding appreciably. The semiconducting element Ge has been investigated in a binary solid solution with Fe (Borg and Lai, 1967). The self diffusion of Fe in this solution was measured and compared to the self diffusion coefficient in pure iron. The coefficients were the same indicating that Ge has no effect on Fe diffusion. In this study then, only carbon in amounts ≥ 0.10 wt% affects the diffusion coefficients for Fe-Ni.

Another possible source of error in the determination of cooling rates is the equilibrium phase diagram used. The Fe-Ni phase diagram has been recently redetermined (Goldstein and Ogilvie, 1965) above 500°C . The solubility limits were extrapolated to 300°C by thermodynamic considerations. The $\alpha/(\alpha + \gamma)$ boundary reached a maximum Ni content in the temperature interval 400 to 500°C . Any error in this boundary would be reflected in the calculation of the kamacite bandwidth especially in meteorites below 7 wt% Ni. Any error in the $\gamma/(\alpha + \gamma)$ boundary would be reflected in the amount of undercooling necessary before nucleation of kamacite. If the error is large the taenite profile would also be changed. The thermodynamics of the Fe-Ni system have recently been evaluated (Rao, Russel and Winchell 1967). They calculated the compositions of the iron-nickel phase diagram and also determined an experimental point at 700°C . Agreement was very good. They also predict that the Ni content at the $\alpha/(\alpha + \gamma)$ boundary reaches a maximum between 400 and 500°C .

The Fe-Ni phase diagram (Goldstein and Ogilvie, 1965) was determined using very pure Fe-Ni samples. As discussed before the iron meteorites typically contain 0.6 wt% Co., 0.17 wt% P, 0.04 wt% S and 0.03 wt% C with trace elements of Co, Cr, Ge, Ga, etc. However, the pure Fe-Ni alloys did contain trace amounts of Cu, Ge (10 - 20ppm) and Cr < 10ppm. The effects of these trace elements can probably be safely ignored. The addition of Co does not shift the $\alpha/(\alpha + \gamma)$, or $\gamma/(\alpha + \gamma)$ phase boundaries significantly (Reed, 1965). Phosphorus, sulfur, and carbon are inhomogeneously distributed mainly in the form of schreibersite or rhabdite, troilite, cohenite or graphite respectively. Although the phase equilibria data on Fe-Ni-P, Fe-Ni-S or Fe-Ni-C are not well known enough to permit any reliable conclusions as to whether the equilibrium Ni contents in kamacite or taenite are changed by the presence of P, S, or C, we may discuss what the effects may be.

According to the Fe-Ni-P phase diagram of Buchwald (1966), which can be considered only tentative, 0.5 wt% P shifts the α and γ solubility boundaries only a few °C for the Ni content range of octahedrites, but considerably more for the Ni range of hexahedrites. Most of the large phosphides, not found within kamacite bands, formed before the Widmanstätten pattern nucleated. Presumably because the diffusion rate of P is so much faster than that for Fe-Ni (Barrer, 1951) much of the P is contained in schreibersite before the Widmanstätten pattern formed. The P content in taenite at these temperatures is probably low, < 0.2 wt%, and has little effect on the phase boundary compositions. A similar argument can be given for the sulfur.

Brett (1966) used projected Fe-Ni-C metastable phase equilibria to show that carbon depresses the $\gamma/(\alpha + \gamma)$ boundary about 10°C per 0.1% C and suggested that this might account for some of the undercooling required by our

model. However, the average C content of typical irons in which inclusions of cohenite, graphite, and cliftonite were purposely avoided is 0.03 wt% (Krinov 1960, and Table 10). The alloys used for phase diagram determination had about 0.01 wt% C or less. For most meteorites and presumably for Group IIIa, IIIb and IVa meteorites which are free of C containing inclusions, the effect of C content is not significant and the Fe-Ni binary diagram can be used. For meteorites in Group I and those which contain cohenite some undercooling is caused by the presence of carbon.

If the effects of C and P were serious then certain systematic errors in cooling rates might be expected. However, this does not occur. For example in Group IIIb, the P level is high and the C level is low; while in Group I, both the P and C levels are high. The cooling rates in both these groups do not vary with Ni or C content. Probably the carbon in Group I is tied up in cohenite rather than influencing the kamacite - taenite equilibrium. This indicates that the measured differences in cooling rates are real and not due to variations in carbon or phosphorous.

The absolute value of the cooling rate can only be determined within a factor of two since there are inaccuracies in the extrapolated diffusion coefficients, and the measured phase diagram. Our interest in this study is to measure differences in cooling rates between various meteorites. The possible errors in diffusion coefficients and phase equilibrium have a much more serious effect on the absolute number than on the variation between meteorites.

The precision of the cooling rate analysis is dependent on the accurate measurement of bandwidth and Ni content. For almost all the samples studied

we were able to measure the kamacite bandwidth to about $\pm 10\%$ with a high degree of confidence. A variation of this amount represents an error in the cooling rate of about $\pm 25\%$. The Ni contents measured by various investigators for the same meteorite usually agree within $\pm 2-3\%$ rel. This represents a deviation in cooling rate of less than 25% . The precision errors are therefore small ($< \pm 50\%$).

In Figure 9 we have plotted the measured bandwidths for meteorites in Ga-Ge Groups I, IIIa, IIIb and IVa vs. their Ni contents. Curves of band-width vs. Ni for constant cooling rates of 1.5, 2.5, 7.5, and $100^\circ\text{C}/\text{m.y.}$ are also included. In Groups I and IIIb the measured bandwidths decrease continuously as the Ni increases and parallel the $2.5^\circ\text{C}/\text{m.y.}$ curves respectively. In Groups IIIa and IIIb, the measured bandwidths are independent of Ni content crossing isocooling curves rather than paralleling them. In these two groups the constancy of bandwidth is due to a variation in cooling rate throughout the groups. The only way, for example, that a member of Group IVa containing 9.8 wt% Ni and the same bandwidth as a member with 7.5 wt% Ni could cool at $100^\circ\text{C}/\text{my}$, would be for the kamacite phase to nucleate without any undercooling. This clearly does not happen. The measurements of cooling rate variations in Groups IIIa and IVa are real and cannot be explained by effects of trace elements or other factors.

Cooling Rates and the Evidence for Several Meteorite Parent Bodies

For many years investigators of meteorites believed that they were produced in molten and differentiated interiors of some earth-like body and that the meteorites which we have collected represents a cross section of some single primordial body (Brown and Patterson, 1948; Uhlig, 1954; Ringwood and Kaufman, 1962). The presence of diamonds in several meteorites suggested bodies

about the size of the moon (Urey, 1956). Many of the properties of meteorites seem to be quantized, Ga-Ge groups and the clustering of olivine compositions in ordinary chondrites for example, and can apparently be most easily explained by separate parent bodies (Anders, 1964). Many investigators now believe that the meteorites formed in relatively small bodies probably located within the asteroid belt.

The cooling rate data helps place boundary conditions on the type of parent body or bodies in which the iron meteorites formed. Since the cooling rates of the iron meteorites are very slow ($< 0.005^{\circ}\text{C}$ per year) they must have been thermally insulated within a large body during the formation of the Widmanstätten pattern. A variation in the cooling rate of three orders of magnitude ($0.4\text{--}500^{\circ}\text{C}/\text{m.y.}$) cannot be obtained in the core of a single meteorite parent body surrounded by silicate material since temperature gradients in the metal will be small (Goldstein and Ogilvie, 1965). If the iron meteorites developed in a single parent body, then they were distributed radially throughout. Evidence for a multiplicity of parent bodies is provided by the Ga-Ge contents and cooling rate data. Because of the quantized nature of the Ga-Ge groups (Goldberg, 1951, Lovering, 1957), it is hard to explain how the iron meteorites formed in a single region of a parent body. Therefore, the meteorites in each Ga-Ge group formed at least in different regions of one, or in several parent bodies. If the Ga-Ge groups formed in one body, then meteorites of the same Ni content had to form in different areas of the parent body since their cooling rates and Ge contents differ by more than an order of magnitude. Also, meteorites with the same cooling rate, and therefore the same position radially within the parent body, had to form in different

regions since their Ni and Ge content differ by large amounts (Figure 7). Therefore, the iron meteorites probably formed in more than one parent body.

The maximum size of any of these parent bodies can be estimated from values of the internal pressures or from the slowest cooling rates. From recent work (Anders, 1964, Goldstein and Ogilvie 1965, Anders et al. 1966, Brett, 1966, Heymann et al., 1966 and Brett and Higgins 1967), there is good reason to believe that the internal pressures in these parent bodies were low ($< 4\text{kb.}$). If a parent meteorite body has a density close to that of chondritic material the radius of the body sustaining such a pressure is no more than 500 km.

Cooling rates can be used to estimate the sizes of parent bodies. Because of the necessity for assumptions as to their composition, thermal conductivity,

radial distribution of material and breakup history, the sizes are only estimates. However, a model can be formulated which may represent one cooling history of the meteorite parent bodies which seems reasonable and self consistent with the data under discussion. Assuming that slow cooling commenced upon solidification of metal and, that the parent body is composed mainly of silicate with the concentration of long-lived radioactivities present in chondrites, temperature-time curves and cooling rates have been calculated (Wood, 1964, Goldstein and Ogilvie, 1965). The cooling rates obtained for different sized parent bodies (Goldstein and Short, 1967) are plotted in Figure 10. The cooling rate varies with temperature. Therefore, for comparison purposes a temperature of 500°C was selected. Also shown in this figure are the cooling rates for iron meteorites found at a distance (r) from the center of the body with radius a , where r/a increases from 0 to 1 proceeding from the center of the body to the outside surface. Other cooling models can be proposed. However, as long as the iron coexists with silicate-like material (Lovering, 1962) the cooling rates for a given sized parent body will be substantially the same ($\pm 50-100\%$).

The cooling rate distribution for the iron meteorites has a sharp lower limit at 0.4°C/my. If meteorites with the lowest cooling rate (0.4°C/my) formed in the core of a parent body the maximum sized body would be about 300 km in radius. Only a few asteroids presently are larger than 300 kms, notably the largest, Ceres, with a radius of 385 km. If meteorites with a cooling rate of 0.4°C/m.y. did not form in the core of a parent body, then the parent body would have to have had a radius larger than 300 km. The fastest cooling rates, over 500°C/m.y., require that the parent body must be smaller than 20 km in radius if

these meteorites formed in the core. The boundary conditions for iron meteorite formation are therefore: 1) more than one parent body, 2) formation with $P < 4$ kb, and 3) maximum size 300 km radius, if the meteorites formed in a core with a silicate mantle.

Relation of Physical and Chemical Properties of Iron Meteorites

Before considering the major question — the number of parent bodies and the distribution of metal within these bodies — we propose to investigate meteorites which are related by their physical and chemical properties. The more properties that relate one meteorite to another, the stronger is the evidence that these meteorites are genetically related. Goldberg (1951) and Lovering (1957) first pointed out that the Ga-Ge contents of most iron meteorites fall into sharply defined clusters, instead of forming a continuous distribution.

Voshage (1967), has shown that the cosmic ray exposure ages of meteorites also correlate in several of the Ga-Ge groups. We have introduced two new interconnected parameters, cooling rate and bandwidth, which are also correlated within the Ga-Ge groups (Figures 7 and 9). These correlations further strengthen the evidence that the meteorites in the Ga-Ge groups are related and reinforce the proposition that, each correlated group comes from a different parent body.

The variation of Ge and Ni within each of the Ga-Ge groups has been used by Wasson (1967a) to determine which meteorites belong to his newly defined groups. Of the meteorites we have studied, 78 (40%) are members of Wasson's defined groups, and 42 (22%) are non-members (Table 12). These 42 meteorites do not fall into recognized groups on the basis of their Ga-Ge and Ni contents.

Ga-Ge-Ni values have not been determined for the other 73 (38%) meteorites in our sample. As shown in Table 11, parameters such as cooling rate, exposure age, bandwidth and plessite structure correlate with Ni content. These correlations, although less definitive than the Ge-Ni correlation, can be used to select possible members of the 5 groups. Based on these criteria, 13 of the remaining 73 unclassified meteorites do not qualify as possible members of the recognized groups and are referred to as non-members (Table 12). The other 60 meteorites, based on the above criteria, are possible members of Ga-Ge Groups I, IIIa, IIIb and IVa (Tables 13-17). If all 60 meteorites prove in the future to be members of the Ga-Ge groups, a large majority (71%) of the iron meteorites studied would fall within the 5 groups.

The cooling rates and Ni contents of all the non-member and possible-member meteorites are shown in Figure 11. The cooling rate - Ni boundaries of the 5 Ga-Ge groups are also included. A line representing a bandwidth of 0.25 mm is also drawn across the cooling rate - Ni distribution. Half the non-member meteorites have bandwidths less than 0.25 mm and fall on the right hand side of this line. These meteorites, the finest octahedrites, transitional octahedrites, and ataxites, have the largest variation in chemical composition and cooling rate and have the fastest average cooling rate of all the groups.

Several meteorites were found to be possible members of both Groups IIIa and IIIb, (Table 16). Their Ni content ranges from 8.5 - 8.9 wt% and their cooling rate between 1 and 2°C/my. This region in the cooling-rate Ni distribution graph (Figure 11) is the area where the transition between IIIa and IIIb occurs. Extrapolation of the bandwidth or cooling rate data vs. Ni from the high Ni end of group IIIa or the low Ni end of group IIIb falls in this area. A transitional

plessite structure showing decomposed plessite as well as kamacite in a Widmanstätten pattern was found in these meteorites. The interesting possibility that IIIa and IIIb are not separate groups but are interconnected will be explored later.

Accepting the probability that the meteorites listed in Tables 13-17 are members of the defined groups, a breakdown of the possible members and non-members of the Ga-Ge groups by textural classes is given in Table 18. Except for meteorites with bandwidths less than 0.25mm, a very large percentage of all the irons studied are probably members of defined Ga-Ge groups.

The Number of Parent Bodies and the Distribution of Iron Meteorites

Two theories have been proposed to explain the formation of iron meteorites in asteroidal sized parent bodies. One theory may be called the core model (Fish, Goles, and Anders, 1960) in which a molten Fe-Ni core is obtained by the melting of material of chondritic composition due to short lived radioactive isotopes, or some other mechanism. In this model, iron meteorites were formed by fusion and differentiation within the parent bodies. The amount of Fe-Ni is usually less than 20% by weight, 10% by volume, in chondrites (Mason, 1962). If complete differentiation occurs, the iron-nickel core will extend no more than $r/a = 0.5$ from the center. From Figure 10 we can see that all the irons in this parent body will have about the same cooling rate. The second model was proposed by Urey (1956) and Henderson and Perry (1958) who suggested that the irons were scattered over the entire volume of the parent body as molten areas ("raisin bread" model). The distribution of raisins was not specified. However, these areas should have had widely differing cooling rates depending upon their burial

depth. Levin (1965) believes that the parent bodies are structured like a "raisin bread" but unlike Urey, he assumes the raisins, iron inclusions, were never molten (Levin raisin bread model). We suggest that irons have been formed in both types of asteroidal bodies.

As discussed in the last section, a large percentage of the iron meteorites in our study can be catalogued into the 5 Ga-Ge groups. The existence of these closely knit groups is good evidence for believing that members of each group are genetically related. A very interesting question is whether we should associate each group with a different parent body. Wasson and Kimberlin (1967c), have argued that it would seem very unlikely that the processes which formed the iron meteorites within their parent bodies could produce two or more discrete groups which are located in contiguous regions. Also the differing Ge-Ni correlations for the several groups argues against more than one body/group. They suggest that the simplest and most reasonable explanation is that each group originated in a separate body. Therefore at least 5 parent bodies are necessary. Wasson supports the core model and would explain the variation of Ga-Ge-Ni within the group by fractional crystallization throughout the core.

If meteorites of a single group form in a core, then the cooling rates should be similar. Only Group I and Group IIIb qualify as possibilities. Group I meteorites cooled between $2-3^{\circ}\text{C}/\text{my}$ and Group IIIb meteorites cooled between $1-2^{\circ}\text{C}/\text{my}$ and their cooling rates are independent of Ni content. The radius of the parent asteroids which contained these irons, based on their cooling rates, was about 175 km for Group I and 210 km for Group IIIb. The meteorites in both groups are similar in many ways. Their Ge contents decrease with increasing

Ni, their plessite structures are similar, (on differing scales) and they contain large numbers of inclusions (phosphides, troilite). Generally the phosphorus contents of the metal areas, excluding large inclusions are between 0.2-0.4 wt% (Moore, and Lewis 1967) (Tables 5 and 7).

Little information is available on the mechanism of core formation. However, separation of metal and silicate is relatively easy as long as the viscosity of the silicate is not too high (Fish, Goles and Anders 1960). Ga-Ge groups I and IIIb have the slowest cooling rates of the 5, and formed in larger parent bodies. The variation of Ni content throughout the groups is usually explained by fractional crystallization in the core (Lovering 1957). However, in laboratory solidification experiments (Goldstein, 1967), the Ge follows the Ni contrary to the Ni-Ge trends found for these groups. Preliminary experiments with Fe-Ni-Ge alloys containing up to 1 wt% phosphorus, which lowers the melting point about 50°C (Hansen, 1958), shows no change in the Ni-Ge distribution. The group I meteorites contain large amounts of carbon in the form of cohenite (Brett, 1966), but the Group IIIb meteorites do not. Evidently the effect of C on crystal fractionation is small. These trends must be explained in considering a core formation mechanism.

The members of Groups IIIa and IVa have differing cooling rates, decreasing with increasing Ni content. All the meteorites in each group could not have formed in the core of one parent body since thermal gradients in the liquid metal will be small (the ratio of the thermal diffusivity of metal to silicate is greater than 10 to 1). Two possible models can be proposed to explain the differing cooling rates within each group. The member meteorites of each group may have

formed either in the cores of parent bodies of differing size, but similar composition, or in different regions within one parent body (raison-bread model). At this time, both models have their drawbacks.

Within each Ga-Ge-cooling rate group there may be sub-groups of meteorites with similar cooling rates. For example, one sub-group might be the low-Ni, fast cooling ($50-90^{\circ}\text{C}/\text{m.y.}$) meteorites in Group IVa (Figure 7). Meteorites in this group may have come from as few as two asteroids. The possible number of sub-groups in IIIa is hard to estimate. Although the separation of irons into a core is favorable (Fish, Goles and Anders, 1960), it is hard to understand how several parent bodies would form each with largely the same chemistry, accumulating at perhaps similar distances from the sun, and yet have very different radii.

If meteorites are to form in different regions of one parent body, incomplete segregation of metal and silicate must occur. The pallasites are probably an example of one group of meteorites which form by such a process. Small crystals of homogeneous olivine each of similar composition are intermixed with Fe-Ni. These meteorites have slow cooling rates ($0.4-2.5^{\circ}\text{C}/\text{m.y.}$) with the vast majority between 0.4 to $1^{\circ}\text{C}/\text{m.y.}$ (Goldstein and Short, 1967, Buseck and Goldstein, 1967). These cooling rates are lower than those of the majority of the irons. In fact only a few irons, about 10% of our sample, have cooling rates which are as low. This result argues strongly against the simple radial distribution model (irons-pallasites-chondrites) since there are few meteorites which have cooling rates low enough to be from the core of the parent body in which the pallasites developed. It is probable therefore that parent bodies have different radii and may undergo differing amounts of internal heating. Some parent bodies had molten cores and some did not. The pallasites resided either in the core of their own parent body (Buseck and Goldstein,

1967), if the fluid core was turbulent, or at the metal-silicate boundary, if Stoke's law is applicable (Fish, Goles, and Anders, 1960). In the latter case a fairly large pallasite layer could still be formed since the separated olivines are loosely packed within the metal. The mechanism for the formation of segregated metal areas in a parent body will be different from that of the pallasites, however.

One possibility to account for the development of the iron meteorite raisins is solid state coarsening (Levin, 1965). When the original silicate material is heated to temperatures over 1300°C, the number of metal particles decreases while their average size increases. The driving force for the change is the tendency to reduce the overall free energy of the system by reducing the total surface energy. The process requires diffusion of metal from small particles to larger ones through intervening silicate. The final mean particle size (\bar{r}) can be calculated by the theory of diffusion controlled coarsening. The following equation by Wagner (1961), can be used to evaluate whether the process suggested by Levin (1965), is at all reasonable:

$$\bar{r}^3 - \bar{r}_0^3 = \frac{(8\gamma DC_e V_m^2)}{(9RT)} t = kt$$

where

\bar{r}_0 is the mean value of the mean particle size \bar{r} at the onset of coarsening, $\sim 1\text{mm}$; γ is the specific surface free-energy of the particle-matrix interface $\sim 200\text{-}700 \text{ ergs/cm}^2$ (Zackay and Aaronson, 1962), V_m is the molar volume of the precipitate, Fe-Ni $\sim 7 \text{ cc/mole}$. D is the coefficient of diffusion of solute in the matrix silicate $\sim 10^{-11} \text{ cm}^2/\text{sec}$ for olivine (Simkin, 1966). At high temperatures ($T \simeq 1300^\circ\text{C}$) the amount of material transported by grain boundary diffusion

is small relative to diffusion within the grain. C_e is the equilibrium molar concentration of the solute ~ 0.5 mole/cc for 10 wt% Fe in olivine. R has its usual meaning, and

$$k = \frac{8\gamma DC_e V_m^2}{9RT}$$

The value of k is about 10^{-18} cc/sec. In 10^8 years the value of \bar{r} is only about 5mm, much smaller than the size of even the smallest iron meteorites. The process of solid state coarsening cannot produce the size raisins formed in the parent bodies. However, it probably plays an important part during reheating of the iron particles in ordinary chondrites.

Another possibility to account for the development of iron raisins is that of forming molten pools of metal. In the parent body, high phosphorous high-Ni metal, which melts first, may segregate to form in the core while the low phosphorus-low Ni metal which melts later may have had only enough time to agglomerate but not enough time to segregate completely from the surrounding silicate. This would allow for the raisin-bread structure and the general Ni-P-Ge-cooling rate trends in Group IIIa and IVa. However, in this model the silicate matrix must remain solid at about 1400°C in order to prevent segregation of metal from silicate. Since chondritic material may, however, be molten at this temperature, obvious difficulties occur. The authors presently support the raisin bread model over that of the multiple body model. Experimental work on this problem is certainly needed.

It is also possible that Group IIIa and IIIb meteorites are related. The high Ni meteorites in Group IIIa and low Ni meteorites in IIIb tend to overlap in Ni, Ga-Ge, and P content as well as in bandwidth-cooling rate and microstructure

(Table 4). Voshage (1967) found that the cosmic-ray ages for members of Group IIIa and IIIb are very similar and Lipschutz (1967) also found that most Group III meteorites are shocked. If these two groups are related then the IIIb meteorites are in the core of 200 km radius body and the IIIa meteorites are the raisins of metal which were not able to segregate completely from the surrounding material. The chemical trends would be explained by two different fractionation mechanisms, one in the core and one within the body.

Since the meteorites in group IVb are ataxites and the band widths were measured on unoriented samples, the cooling rates could easily vary by a factor of 2 or 3 throughout the whole distribution. It is not clear whether they formed in the core of a parent body or not. About twenty five percent of our sample of iron meteorites do not belong to any of the Ga-Ge groups enumerated to date. Almost half of these meteorites have fine structures with bandwidths less than 0.25mm and most of them cooled faster than the octahedrites with coarser structure. Notable exceptions are Dayton, Follinge, and Tazewell (16-18% Ni) with cooling rates of about $2^{\circ}\text{C}/\text{m.y.}$ and Butler, an unusual iron meteorite (Wasson, Goldstein, 1966) with 2000 ppm Ge and a cooling rate of $0.4^{\circ}\text{C}/\text{m.y.}$ Some of these meteorites may come from the cores of other parent bodies. It is also possible that another Ga-Ge group can be defined on the basis of cooling rate and Ge-Ni variations; 9.8 - 10.9 Ni, 29-130 ppm Ge and $200\text{--}500^{\circ}\text{C}/\text{m.y.}$ (Figure 11). These may be associated with one parent body.

Should a parent body be associated with each meteorite not in a group? This would require at least 50 parent bodies. Probably some irons are end members of large groups (Anoka and Mungindi in IIIb) and others, particularly the meteorites with fine structure and fast cooling rate, may represent the raisins near the

surface of some parent body whose main iron mass is at the center. This would reduce the number of parent bodies.

It is perhaps surprising that we are receiving such a biased sample of meteorites, mainly from only 5 parent bodies. Because of the large number of asteroids, we would expect material from many parent bodies. This circumstance has been explained by Anders (1964) who suggests that we are receiving most of our samples from parent asteroids which are in Mars crossing orbits. Other samples would then come from pieces of asteroids which are propelled by collisions into Mars crossing orbits.

The special position of the asteroid belt on the boundary between the zones of the earth-type planets and the giant planets may explain how parent bodies of differing initial compositions may have developed (Levin, 1965, Larimer 1967, Larimer and Anders 1967). A discussion following Larimer and Anders follows. They propose that the asteroids were produced from a gas of cosmic composition and the metallic elements condense directly from the gas. The iron meteorites are formed in parent bodies essentially composed of two types of condensate, a fine grain dust (Matrix, fraction A) and metal and silicate droplets (Chondrules, fraction B). The depletion of various elements is controlled by the relative amounts of A and B and is reflected in the irons by their Ga and Ge contents. The Ga and Ge are present in fraction A. Therefore Ga-Ge group I has a larger proportion of A in its parent body than does Ga-Ge group III or Ga-Ge group IV. The accretion temperatures and distances from the sun may also have been different for each parent body. This might allow for various subgroups within the Ga-Ge groups as discussed previously. Larimer and Anders also point out that the ordinary chondrites and irons on Ga-Ge groups III agree in both their

condensation temperatures, postulated amounts of fraction A, and similarities in cosmic ray exposure ages. These facts raise the possibility that the ordinary chondrites and the Group III meteorites are genetically related.

Conclusions

We conclude from the measured cooling rate variations (0.4 to 500°C/m.y.) of 193 iron meteorites that, 1) these meteorites formed in more than one body, 2) the Widmanstätten pattern developed at low pressures and, 3) the maximum size of the parent bodies was about 300 km in radius if the meteorites formed in the center of the body. Correlations of bandwidth, and cooling rate versus Ni as well as structural and cosmic-ray exposure age correlations, provide strong evidence that meteorites in the Ga-Ge groups are genetically related.

Meteorites in Ga-Ge groups I and IIb, with cooling rates of 2-3°C/m.y. and 1-2°C/m.y. respectively, probably formed in the cores of parent bodies about 200 km in radius. Meteorites in Groups IIIa and IVa, with cooling rates varying from 1.5-10°C/m.y. and 7-90°C/m.y. respectively, probably formed in areas spread out throughout the whole radius of their parent bodies. These areas were molten at one time during their formation. It is concluded that we are receiving most of the iron meteorites from only a few parent bodies.

Acknowledgements

We wish to thank P. Soules for his assistance with the experimental part of the investigation and J. Wasson and E. Anders for their valuable suggestions and criticisms. We are very grateful to R. Clarke of the National Museum and C. B. Moore of the Ninninger collection at Arizona State University for the loan of so many of their iron meteorites. We also wish to thank R. Clarke, J. Wasson, C. B. Moore, C. Lewis and M. Hey for allowing us to use their chemical analyses prior to publication. One of us (J. M. S.) was supported by a National Academy of Sciences Resident Research Associateship at the Ames Research Center.

LIST OF TABLES

	<u>Page</u>
Table 1 - Measured Band Widths, Ni Contents and Cooling Rates for 193 Octahedrites, Transitional Octahedrites and Ataxites with Ni Contents from 7 to 30 wt % Ni	10
Table 2 - Textural Classification of the Irons	20
Table 3 - Cooling Rate Variations within the Textural Classes.	21
Table 4 - Resolved Ga-Ge-Ni Groups	22
Table 5 - Iron Meteorites in Group I.	24
Table 6 - Iron Meteorites in Group IIIa	25
Table 7 - Iron Meteorites in Group IIIb	26
Table 8 - Iron Meteorites in Group IVa	27
Table 9 - Iron Meteorites in Group IVb	28
Table 10 - Carbon Contents of Iron Meteorites	32
Table 11 - Summary of Correlations of Various Parameters with Respect to Increasing Ni Content within the Ga-Ge Groups . .	41
Table 12 - Meteorites which Are Not Members of Ga-Ge Groups	42
Table 13 - Possible Members of Group I.	45
Table 14 - Possible Members of Group IIIa	46
Table 15 - Possible Members of Group IIIb	47
Table 16 - Possible Members of Group IIIa-IIIb	47
Table 17 - Possible Members of Group IVa	48
Table 18 - Members and Non-Members of Ga-Ge Groups	49

LIST OF ILLUSTRATIONS

Figure 1. Fe-Ni Phase Diagram, (Goldstein and Ogilvie, 1965). The $\alpha/(\alpha + \gamma)$ and $\gamma/(\alpha + \gamma)$ equilibrium phase boundaries are shown; dashed lines indicate extrapolated values below 500°C. The temperature at which α_2 forms as a function of composition is given by the line labeled M_s . The Ni variations within the textural groups of the iron meteorites are also indicated.

Figure 2. Effect of Impingement. The meteorite considered has 10 wt% Ni, the kamacite bands nucleated at 600°C, 110°C below the $\gamma/\alpha + \gamma$ boundary, and the meteorite cooled at a rate of 1°C/m.y. Kamacite grows to a width of $414\mu(W_\infty)$ when impingement is negligible ($X_0 = \infty$). As long as X_0 is greater than W_∞ , the amount of growth is approximately W_∞ . When X_0 is less than W_∞ , the amount of growth is severely restricted.

Figure 3. Cooling rate of the Widmanstätten structure at 500°C as a function of kamacite plate thickness and bulk Ni content of the meteorite. The nucleation temperature of kamacite is taken to be 110°C below the $\gamma/(\alpha + \gamma)$ boundary in the Fe-Ni phase diagram, and it is assumed that kamacite growth is unimpeded by other impinging kamacite plates.

Figure 4. Bandwidth Distribution for the Edmonton, Kentucky and Mt. Edith Iron Meteorites. The distributions are roughly Gaussian and the average value is used for the meteorite bandwidth.

Figure 5. Bandwidth Distribution for the Iron Meteorites.

Figure 6. Cooling Rate Histogram (total distribution and distribution by textural classes). The cooling rate variations within the 5 Ga-Ge Groups are outlined.

Figure 7. Variation of Cooling Rate and Ni Content for Meteorites in the 5 Ga-Ge Groups. The numbers in parentheses indicate the number of meteorites studied in each group. Each cooling rate-Ge group plots coherently and is outlined on the graph.

Figure 8. Photomicrographs of Plessite Structures in the Ga-Ge groups.

a	Toluca	- Group I
b	Grant	- Group IIIb
c	Spearman	- Group IIIa
d	Bristol	- Group IVa
e	Weaver Mtns.	- Group IVb

Figure 9. Variation of kamacite bandwidth as a function of Ni content for the Ga-Ge groups I, IIIa, IIIb, and IVa. Meteorites in Groups I and IIIb have bandwidths which decrease continuously with Ni content. Meteorites in Groups IIIa and IVa have bandwidths which are independent of Ni content.

Figure 10. Cooling rates for different sized parent bodies normalized to 500°C. The cooling rates are plotted as a function of r/a where r is the distance from the center of the body and a is the radius of the parent body. T_0 is the initial temperature, 2100°K, and α is the thermal diffusivity, 0.007 cm²/sec.

Figure 11. Cooling Rates for Meteorites not designated as members of the Ga-Ge groups. Possible members and nonmembers of the groups are noted. Outlines of the defined cooling rate - Ni groups are also included. A line representing a bandwidth of 0.25 mm is drawn across the cooling rate Ni distribution.

BIBLIOGRAPHY

- Anders, E., (1964), Origin, Age, and Composition of Meteorites, Space Science Reviews 3, 583-714.
- Anders, E., and Lipschutz, M. E., (1966), Critique of Paper by N. L. Carter and G. C. Kennedy, 'Origin of Diamonds in the Canyon Diablo and Novo Urei Meteorites:', J. of Geophys. Res., 71, 645-661.
- Anders, E. (1967), Private Communication.
- Badia, M., and Vignes, A., (1966), Private Communication, Ecole Nationale Supérieure de la Metallurgie et de l'Industrie des Mines, Nancy France.
- Barrer, R., (1951), Diffusion in and Through Solids, Cambridge.
- Borg, R. J. and Lai, D. Y. F. (1967), Diffusion of Fe in Various Dilute Fe Alloys, Presented at the Annual Meeting of the A.I.M.E., Los Angeles, California to be published.
- Brett, R., (1966), Cohenite in Meteorites: A Proposed Origin, Science, 153, 60-62.
- Brett, R., and Higgins, G. T., (1967), Cliftonite in Meteorites: A Proposed Origin, to be published in Science.
- Brown, H., and C. Patterson (1948), The Composition of Meteoritic Matter, J. Geology. 56, 85-111.
- Buchwald, V. F. and Munck, S., (1965), Catalogue of Meteorites, Analecta Geologica I, Mineralogisk Museum, Copenhagen.

- Buchwald, V. F., (1966), The Iron - Nickel - Phosphorous System and the Structure of Iron Meteorites, Acta Polytechnica Scandinavica, Chemistry including Metallurgy Series, No. 51.
- Buddhue, J. D., (1946), The Average Composition of Meteorite Iron, Pop. Astronomy 54, 149.
- Buseck, P. R. and Goldstein, J. I., (1967), Olivine Compositions and Cooling Rates of Pallasitic Meteorites, in preparation.
- Clarke, R., (1967), Private Communication, U. S. National Museum.
- Cobb, J. C., (1967), A Trace Element Study of Iron Meteorites, J. Geophys. Res., in press.
- Fish, R. A., Goles, G. G., and Anders, E., (1960), The Record in the Meteorites III. On the Development of Meteorites in Asteroidal Bodies. Astrophysical Journal, 132, 243-258.
- Goldberg, E. Uchiyama, A. and Brown, H., (1951), The Distribution of Nickel, Cobalt, Gallium, Palladium and Gold in Iron Meteorites, Geochim. et. Cosmochim. Acta 2, 1-25.
- Goldstein, J. I., Hanneman, R. E., and Ogilvie, R. E., (1964), Diffusion in the Fe-Ni System at 1 Atmosphere and 40 Kbars Pressure, Trans. Met. Soc. A.I.M.E. 233, 812-820.
- Goldstein, J. I., and Ogilvie, R. E., (1965), A Re-Evaluation of the Iron-Rich Portion of the Fe-Ni System, Trans. Met. Soc. A.I.M.E., 233, 2083-2087.
- Goldstein, J. I. and Ogilvie, R. E., (1965), The Growth of the Widmanstatten Pattern in Metallic Meteorites, Geochim. et. Cosmochim. Acta 29, 893-920.

- Goldstein, J. I., (1966), Butler, Missouri: An Unusual Iron Meteorite, *Science* 153, 975-976.
- Goldstein, J. I., and Short, J. M., (1967), Cooling Rates of 27 Iron and Stony-Iron Meteorites, *Geochim. et. Cosmochim. Acta* 31, in press.
- Goldstein, J. I., (1967), The Distribution of Ge in the Metallic Phases of Some Iron Meteorites, *J. Geophys. Res.*, in press.
- Hansen, M., (1958), *Constitution of Binary Alloys*, J. Wiley & Sons.
- Henderson, E. P. and Perry, S. H., (1958), Studies of Seven Siderites, *Proc. U. S. National Museum* 107, 339-403.
- Henderson, E. P., (1966), Private Communication, U. S. National Museum.
- Hey, M., (1967) Private Communication, British Museum.
- Heymann, D., Lipschutz, M. E., Neilsen, B., and Anders, E., (1966), Canyon Diablo Meteorite: Metallographic and Mass Spectrometric Study of 56 Fragments, *J. Geophys. Res.*, 71, 619-641.
- Jaeger, R. and M. Lipschutz (1967) Geophysical Implications of Shock Effects in Iron Meteorites, *Geochim. et. Cosmochim. Acta*, this issue.
- Krinov, E. L., (1960), *Principles of Meteoritics*, Pergamon Press, New York, p. 284.
- Larimer, J. (1967), Chemical Fractionations in Meteorites I. Condensation of the Elements, *Geochim. et. Cosmochim. Acta*, 31, in press

- Larimer, J. and E. Anders (1967) Chemical Fractionations in Meteorites II Abundance Patterns and their Interpretation, *Geochim. et. Cosmochim. Acta*, 31, in press.
- Levasseur, J., and Philibert, J., (1966), "Determination des Coefficients de Diffusion Intrinseques par Mesure de L'Effect Kirkendall Das Le Systeme Fer-Nickel Submitted to *Compte Rendue*.
- Levin, B. Yu, (1965), The Origin of Meteorites, *Usp. Fiz, Nauk* 86, 41-69, English Soviet Physics *Uspekhi*, 8, 360-378.
- Lovering, J. F., (1962), The Evolution of the Meteorites - Evidence for the Co-existence of Chondritic, Achondritic, and Iron Meteorites in a Typical Parent Meteorite Body in "Researches on Meteorites," et. by C. B. Moore, J. Wiley and Sons, Inc., N. Y., pp. 179-197.
- Lovering, J. F., Nichiporuk, W., Chodos, A., and Brown, H., "The Distribution of Gallium, Germanium, Cobalt, Chromium, and Copper in Iron and Stony-Iron Meteorites in Relation to Nickel Content and Structure, *Geochim. et. Cosmochim. Acta*, 11, 263-278.
- Lovering, J. F., (1956), Structural and Compositional Studies on Selected Phases of Iron and Stony-Iron Meteorites, Ph.D. Thesis, California Institute of Technology.
- Mason, B., (1962), *Meteorites*, J. Wiley, New York.
- Mason, B., and Wiik, H. B., (1965), Analyses of Eight Iron Meteorites, *Geochim. et. Cosmochim. Acta*, 29, 1003-1005.
- Moore, C. B., and Lewis, C., (1967), Arizona State University, Private Communication.

- Moore, C. B., and Jost, P., (1965), Variations on the Chemical and Mineralogical Compositions of Rim and Plains Specimens of the Canyon Diablo Meteorites, Barringer Meteorite Crater, Arizona, presented at the section on Cosmic Chemistry of the XXth International Congress on Pure and Applied Chemistry, Moscow, U.S.S.R., submitted to *Geochim. et Cosmochim. Acta* (1967).
- Nevin, C. M., (1949), *Principles of Structural Geology*, Wiley, New York, 346.
- Nielan, J., (1966), Private Communication, U. S. National Museum.
- Prior, G. T. and Hey, M. H., (1953), *Catalogue of Meteorites*, 2nd ed. British Museum, London.
- Proschan, F., (1953), Confidence and Tolerance Intervals for the Normal Distribution, *J. Amer. Statistical Assn.*, 48, 550-564.
- Rao, M. M., Russell, R. J. and Winchell, P. G., (1967), A Correlation of Thermodynamic Variables for Iron Rich Iron-Nickel-Carbon Alloys, *Trans. Met. Soc. A.I.M.E.*, 239, 634-642.
- Reed, S. J. B., (1965), Electron - Probe Microanalysis of the Metallic Phases in Iron Meteorites, *Geochim. et. Cosmochim. Acta* 29, 535-549.
- Ringwood, A. E. and L. Kaufman (1962), The Influence of High Pressure on Transformation Equilibria in Iron Meteorites, *Geochem. et. Cosmochim. Acta* 26, 999-1009.
- Sabutier, J. P., and Vignes, A., (1966) Private Communication, Ecole Nationale Supérieure de la Mé'tallurgie et de l'Industrie des Mines, Nancy, France.

- Short, J. M., and Anderson, C. A. (1965), Electron Microprobe Analyses of the Widmanstätten Structure of Nine Iron Meteorites, *J. Geophys. Res.* 70, 3745-3759.
- Short, J. M. and Goldstein, J. I., (1967), Rapid Methods of Determining Cooling Rates of Iron and Stony Iron Meteorites, *Science*, 156, 59-61.
- Simkin, T., (1966), Zoned Olivines and the Cooling History of a Picritic Sill, presented at the GSA meeting, San Francisco, California, November 14.
- Smales, A. A., Mapper, D. and Fouche, K. F., (1967), The Distribution of Trace Elements in Iron Meteorites, as Determined by Neutron Activation, *Geochim. et Cosmochim. Acta*, 31, 673-720.
- Uhlig, H. H., (1954), Contribution of Metallurgy to the Origin of Meteorites I. *Geochim. et Cosmochim. Acta* 6, 282-301.
- Urey, H. C., (1956), Diamonds, Meteorites, and the Origin of the Solar System *Astrophys. J.* 124, 623-637.
- Voshage, H., (1967), Bestrahlungsalter und Herkunft der Eisenmeteorite, *Z. Naturforsch.*, in press.
- Wagner, C., (1961), *Z. Elektrochem.* 65, 581.
- Wasson, J. T., (1966), Butler, Missouri: An Iron Meteorite with Extremely High Germanium Content, *Science* 153, 976-978.
- Wasson, J. T., (1967a), Chemical Definition of Genetic Groups of Iron Meteorites, Submitted to *Science*.

- Wasson, J. T., (1967b), The Chemical Classification of Iron Meteorites: A Study of Iron Meteorites with Low Concentrations of Gallium and Germanium, *Geochim. et Cosmochim. Acta.* 31, 161-180.
- Wasson, J. T., and Kimberlin, J., (1967c), The Chemical Classification of Iron Meteorites – 2. Irons and Pallasites with Germanium Concentrations Between 8 and 100 ppm, *Geochim. et. Cosmochim. Acta*, to be published.
- Wells, C., and Mehl, R. G., (1941), Rate of Diffusion of Nickel in Gamma Iron in Low-Carbon and High-Carbon Nickel Steels, *Trans. Met. Soc. A.I.M.E.*, 145, 329-338.
- Wood, J. A., (1964), The Cooling Rates and Parent Planets of Several Iron Meteorites, *Icarus* 3, 429-459.
- Zackay, V. F., and Aaronson, H. I., (1962), *Decomposition of Austenite by Diffusional Processes*, J. Wiley, New York.

Table 1
Cooling Rates of the Irons

Name of Meteorite	Structure	Kamacite Band Width (mm)	Ni Content (wt. %)	Cooling Rate ($^{\circ}\text{C}/\text{my}$)
Abancay	Om	0.55	7.94(M)	15
Aggie Creek	Og	1.2	8.54(E.P.H.), 8.45(W)	1.5
Altonah	Of	0.35, 0.36 (L)	8.64(G)	18
Annahmeim	Og	1.5	7.50 (Cobb)	3
Anoka	Of	0.33	11.75(M), 11.94(W)	1.5
Apoala (pseudo)	Om	0.85	8.2(M), 8.23(W)	4
Arispe	Ogg	2.3	6.97(G), 6.5(W)	> 2
Arlington	Om	0.5	8.55(C)	8
Arltunga	Off-D	~0.005	10.08(L)	> 500
Ashfork (Canyon Diablo)	Ogg	2.5	7.0(W), 7.04(M&W)	2
Bacubirito	Off-D	~0.07	9.8(M)	~200
Bagdad	Og	1.1	7.8(M)	5
Bahjoi	Og	1.3	7.35(Cobb)	3.5
Ballinoo	Off-D	~0.08	10.06(L), 9.7(W), 9.8(H)	~200
Bartlett	Og	1.1	8.9(E.P.H)	1.5
Basedow Range	Og	1.0	7.42(L)	7
Bear Creek	Om	0.75	10.02(G), 9.65(M), 9.99(W)	1.2
Bear Lodge	Og	1.1	7.88(M)	4
Bella Roca	Om	0.75, 0.45	9.95(M), 10.16(W)	1-2
Billings	Og	1.3	7.91(M)	3

Table 1 (Continued)
Cooling Rates of the Irons

Name of Meteorite	Structure	Kamacite Band Width (mm)	Ni Content (wt. %)	Cooling Rate (°C/my)
Bischtübe	Og	1.5	8.0(W)	2
Bishop Canyon	Of	0.3	7.9(W)	65
Bodaibo	Of	0.3	8.05(C)	60
Bogou	Og	1.8	6.92(Cobb), 7.2(W)	3
Bohumilitz	Og	1.9	7.45(W), 7.2(H)	2
Boxhole	Om	0.8	7.72(L), 7.65(W)	8
Breece	Om	0.85	9.64(W), 9.16 (E.P.H.)	1.2
Brenham Township	Om-P	0.95	10.98(L), 11.1 ± 0.5(W)	0.4
Briggsdale	Og	1.2	8.25(M)	2
Bristol	Of	0.3	8.2(G), 8.2(H)	50
Bugaldi (Boogaldi)	Of	0.4(L)	8.99(L)	10
Butler	Off-D	0.15	16.0(W)	0.4
Cacaria	Og	1.0	7.74(C)	6
Cambria (Lockport)	Om	0.65	10.1(W), 10.5(H)	1.5
Campbellsville	Og	1.25	8.57(M)	1.0
Canton	Og	1.0	7.69(M&W)	5
Canyon City	Og	1.0	7.78(W)	5
Canyon Diablo #1	Og	1.9	7.11(G), 7.23(M), 7.2(W)	2.5
" #2	Og	1.24	8.22(G), 8.19(M), 7.93(W)	2.5
" #3	Og	1.19	8.2(W), 8.19(M)	2.2

Table 1 (Continued)
Cooling Rates of the Irons

Name of Meteorite	Structure	Kamacite Band Width (mm)	Ni Content (wt. %)	Cooling Rate ($^{\circ}\text{C}/\text{my}$)
Cape of Good Hope	D	~ 0.03	16.48(G), 16.1(H)	~ 7
Cape York	Og	1.8	7.65(M), 7.47(W)	2
Carbo	Om	0.8	9.98(W)	1
Carlton	Off	0.15	12.68(G), 13.02(W)	3
Carthage	Og	1.2	8.37(W)	2
Casimiro de Abreu	Og	1.2, 1.4	8.5(M)	1.5
Casas Grandes	Og	1.05	7.9(C), 7.8(W)	4
Charcas	Om	0.9	8.17(M)	4
Charlotte	Of	0.4	8.19(Cobb), 8.13(W)	18
Chihuahua City	Ogg	~ 7	6.85(G)	< 1
Chile	Of	0.35	7.66(M)	70
Chilkoot	Og	1.0	7.89(G)	4
Chinaulta	Of	0.35	9.78(W), 9.3(H)	8
Chinga	D	~ 0.015	16.5(Nielan)	~ 25
Chupaderos	Om	0.6	10.4(W)	1.2
Clark County	Og	1.2	7.02(G), 6.9(M), 7.27(Cobb)	8
Cleveland	Og	1.0, 1.12	8.90(M), 8.9(W)	1.5
Concepcion	Om	0.58	9.97(M)	1.5
(May be the same as Chupaderos)				

Table 1 (Continued)
Cooling Rates of the Irons

Name of Meteorite	Structure	Kamacite Band Width (mm)	Ni Content (wt. %)	Cooling Rate (°C/my)
Coopertown	Og	1.5, 1.72	8.47(M)	1.2
Costilla Peak	Og	1.0	7.53(G), 7.55(M), 7.55(W)	7
Cowra	D	0.075	13.72(L), 12.3(W)	7
Cranbourne (Langwarrin)	Ogg	~2	7.1(L), 7.0(W)	3
Cruz del Aire	Om	0.65	9.19(C)	3
Cuernavaca	Om	0.6	10.4 ± 0.5(W)	1.3
Cumpas	Og	1.15	8.14(C)	2.2
Dayton	Off-D	~0.035	18.1(E.P.H. & Perry)	2
Deep Springs	D	~0.01	13.4(Cobb)	~400
Delegate	Om	0.9, 0.7	9.34(L), 9.8(W)	1.2
Deport	Og	1.5	8.4(G)	1.0
Descubridora	Og	1.15	7.7(W)	4
Drum Mtns.	Og	1.1	8.31(W)	2
Duchesne	Of	0.25	9.49(W)	12
Duel Hill (1854), Jewel Hill	Of	0.42	10.2 (M)	3
Edmonton, Kty.	Of	0.28	12.68(G), 12.66(W)	1.0
El Capitan	Og	1.0	8.8(C)	1.8
Elbogen	Om	~0.8	10.25(C)	~0.8
Föllinge	Off	0.04	18.0(B)	1.5

Table 1 (Continued)
Cooling Rates of the Irons

Name of Meteorite	Structure	Kamacite Band Width (mm)	Ni Content (wt. %)	Cooling Rate ($^{\circ}\text{C}/\text{my}$)
Franceville	Og	1.0	8.32(W)	3
Gibeon	Of	0.35	7.96(L)	50
Glorieta Mtn.	Om-P	0.85	11.79(E.P.H.), 12.04(W)	0.4
Goose Lake	Og	1.2	8.25(M), 8.48(G), 8.39(E.P.H.)	2
Grand Rapids	Om	0.55	9.38(E.P.H.), 9.41(W)	3
Grant	Om	0.8	9.29(W)	1.5
Gun Creek	Om	0.75	8.46(W)	4
Gundaring	Om	0.8(L)	8.32(L)	4
Hammond Township	Om	0.7	8.18(W)	7
Harriman	Om	0.95	7.86(E.P.H.)	5
Henbury	Om	0.9	7.59(G), 7.47(W)	8
Hill City	Of	0.37	9.32(G), 9.21(E.P.H.)	10
Hoba	D	~ 0.03	~16.2(Prior)	~9
Hualapai (Wallapai)	Of	0.35, 0.44	11.6(W)	1.0
Huizopa	Of	0.3	7.81(L), 7.8(H)	65
Illinois Gultch	D	~ 0.05	12.4(H)	~40
Iquique	D	~ 0.01	15.99(E.P.H.)	~ 80
Jamestown	Of	0.30	7.54(W), 7.6(H)	90
Joe Wright Mtn.	Om	0.95, 0.93	9.21(M)	1.5
Karee Kloof	Og	~ 1.7	7.68(W)	~2
Kenton County	Om	0.85	7.52(M)	8

Table 1 (Continued)
Cooling Rates of the Irons

Name of Meteorite	Structure	Kamacite Band Width (mm)	Ni Content (wt. %)	Cooling Rate ($^{\circ}\text{C}/\text{my}$)
Kingston	Om	0.9	7.0(M)	12
Klondike	D	~ 0.01	~ 18.2 (Prior)	20
Knowles	Om	0.88	8.59(M&W), 9.3(W)	1.5
Kokomo	D	~ 0.06	16.2(W)	~ 2
Kyancutta	Og	1.14	8.28(L)	2
La Grange	Of	0.33	7.71(G)	70
Laurens County	Of	0.35	~ 13.4 (M.P.A.)	~ 0.5
Leeds	Og	1.2	8.08(G)	2
Lenarto	Og	1.3	8.7(M)	1
Lexington County	Ogg	2.0	7.45(E.P.H.)	2
Livingston (Tennessee)	Og	1.0	7.45(E.P.H.)	7
Loreto	Og	1.2	7.9(M), 7.75(E.P.H.)	3.5
Madoc	Om	0.8	7.66(W)	10
Maria Elena (1935)	Of	0.3	7.76(G), 7.65(W)	70
Mart	Of	0.4	9.3(M)	7
Mazapil	Og	1.0	8.42(Cobb)	2.5
Mbosi	Om	0.8	8.88(W)	2
Merceditas	Og	1.0	7.93(W)	4.5
Mertzon	Om	0.9	9.6(E.P.H.)	1
Monahans	Off-D	~ 0.025	11.9(Cobb), 10.6(H), 10.8(C)	~ 500
Moonbi	Om	0.55	7.99(L)	12

Table 1 (Continued)
Cooling Rates of the Irons

Name of Meteorite	Structure	Kamacite Band Width (mm)	Ni Content (wt. %)	Cooling Rate ($^{\circ}\text{C}/\text{my}$)
Mooranoppin	Ogg	~2	6.91(L)	~3.5
Morito	Om	0.96	7.67(G)	7
Morradal	D	~0.01	~18.8(Prior)	~15
Mt. Edith	Om	0.75	9.4(L), 9.1 \pm 0.5(W)	2 \pm 0.5
Mt. Magnet	Off-D	0.02	14.72(L)	50
Mt. Stirling	Ogg	2.4	6.93(L)	3
Mungindi		0.33	12.2(L)	2
Narraburra	Om	0.5(L)	10.22(L)	2
Nativitas (Santa Apolonia)	Og	1.02	7.83(G), 7.45(W)	7
Nejed	Of	0.30	7.78(M)	70
Nelson County	Ogg	~5	6.8(E.P.H.), 6.93(W)	~0.8
New Westville	Of	0.40	9.38(C), 9.48(W)	7
Norfolk	Og	1.05, 1.20	7.51(M&W), 7.49(W)	6
Norfolk	Om	0.9	7.88(W), 7.95(M)	5
Obernkirchen	Of	0.25	7.67(C)	100
Odessa	Og	1.6	7.55(G), 7.5(W)	3
Ogallala	Og	1.7	8.1(W)	1.0
Orange River (iron)	Og	1.5	8.62(M)	1.0
Otchinjua	Of	0.35	8.0(H)	50
Owens Valley	Og	1.15	8.66(M)	2

Table 1 (Continued)
Cooling Rates of the Irons

Name of Meteorite	Structure	Kamacite Band Width (mm)	Ni Content (wt. %)	Cooling Rate ($^{\circ}\text{C}/\text{my}$)
Pará de Minas	Of	0.38	8.12(Cobb), 8.18(M), 8.04(W)	25
Perryville	Off-D	0.06	9.8(M)	250
Persimmon Creek	Off	0.06	13.6(Nielan)	10
Piñon	D	~ 0.02	16.58(G)	~ 12
Pitts	Of	0.27	13.0(Cobb)	0.8
Plymouth	Og	1.05	8.69(M)	2
Providence	Og	1.2	8.28(W)	2
Puente del Zacate	Om	0.99	8.21(G)	3
Putnam County	Of	0.3	$\sim 7.9(\text{Prior})$	~ 60
Red River	Om	0.92	9.8(M)	0.8
Richa	Om	0.95	8.7(H)	2
Rifle	Og	1.9	7.3(M)	2
Rodeo	Om	0.55, 0.47	9.44(W), 10.5(M)	2-3
Roebourne	Og	1.25(L)	8.04(L)	2.5
Roper River	Om	0.75	9.91(L), 9.81(W)	1.2
Ruff's Mountain	Of	1.1	8.65(W)	1.5
Sacramento Mtn.	Og	1.01	7.75(W)	5
St. Genevieve County	Of	0.45	7.96(C)	20
Samelia	Og	1.2	8.03(Cobb)	3
Sams Valley	Om	0.8	9.91(W)	1.0

Table 1 (Continued)
Cooling Rates of the Irons

Name of Meteorite	Structure	Kamacite Band Width (mm)	Ni Content (wt. %)	Cooling Rate ($^{\circ}\text{C}/\text{my}$)
San Angelo	Om	0.85	7.6(M), 7.68(W)	7.5
Sanderson	Om	0.75	9.27(G), 9.66(W)	1.2
Seneca Township	Of	0.45	8.52(W)	12
Shingle Springs	D	~ 0.01	17.0(W)	~ 50
Social Circle	Of	0.35	7.44(E.P.H.), 7.58(W)	70
South Byron	D	~ 0.01	18.2(W)	~ 20
Spearman	Om	0.9, 1.06	8.72(W)	2
Staunton	Og	1.45	8.8(M)	1.0
Tamarugal	Og	1.0	8.44(W)	2
Tambo Quemado	Om	0.75	9.89(E.P.H.), 10.12(W)	1.2
Tawallah Valley	D	~ 0.01	18.21(L)	~ 20
Tazewell	Off	0.05	16.7(G)	2
Thunda	Og	1.64	8.27(L)	1.2
Thurlow	Om	0.8	9.92(W)	1.0
Tieraco Creek	Om	0.5	10.55(L), 10.72(W)	1.5
Tlacotepec	D	~ 0.03	~ 16.2 (Prior)	~ 8
Toluca	Og	1.1	8.31(G), 8.08(W)	2
Tonganoxie	Og	1.25	7.8(M)	3.5
Trenton	Om	0.95	8.34(W)	2.5

Table 1 (Continued)
Cooling Rates of the Irons

Name of Meteorite	Structure	Kamacite Band Width (mm)	Ni Content (wt. %)	Cooling Rate ($^{\circ}\text{C}/\text{my}$)
Treysa	Om	0.95	8.62(Cobb), 9.1(W)	1.5
Twin City	D	~0.001	29.91(Mason)	~0.8
Verkhne Dnieprovsk	Om	0.75	9.86(W)	1.2
Victoria West	Of	0.35	11.7(W)	1.2
Weaver Mtns.	D	~0.01	18.0(E.P.H. & Perry)	~20
Western Arkansas	Of	0.35	7.70(W)	65
Wiley	Off-D	0.05	11.71(E.P.H.), 11.8(W)	65
Willamette	Og	~1.0	7.62(W)	~6
Williamstown	Om	0.85	7.56(M), 7.52(W)	10
Willow Creek	Og	1.41	8.75(G)	1.0
Wonyulgunna	Om	0.8	9.05(L)	2
Woodbine	Of	0.3	~12.6(M.P.A.)	1
Yanhuitlan	Of	0.35	7.5(W)	80
(Pseudo Misteca)				
Yenberrie	Og	1.9	6.97(L), 7.0(E.P.H.)	3
Youndegin	Ogg	~2.5	6.92(L)	~2

References for Table 1

- (M) Moore and Lewis, (1967) (L) Lovering, (1956) - Kamacite Bandwidth (Nielan) Nielan, J. (1966)
(E. P. H.) Henderson, (1966) (L) Lovering, et. al (1957) (E. P. H. & Perry) Henderson and Perry (1958)
(W) Wasson, (1967a, b, c) (M & W) Mason and Wiik (1965) (B) Buchwald, (1966)
(G) Goldberg, (1951) (Cobb) Cobb, (1967) (Prior) Prior and Hey (1953)
(C) Clarke, (1967) (H) Hey, (1967) (M. P. A.) Microprobe Analysis of Plessite

Table 2
Textural Classification of the Irons (Buchwald and Munck, 1965)

Structure Type	Band Width (mm)
Extremely Coarse Octahedrites (Oge)	>4.0
Coarsest Octahedrites (Ogg)	2.0-4.0
Coarse Octahedrites (Og)	1.0-2.0
Medium Octahedrites (Om)	0.5-1.0
Fine Octahedrites (Of)	0.25-0.50
Finest Octahedrites (Off)	<0.25
Transitional Octahedrites (Off-D)	<0.25
Ataxites (D)	<0.25

Table 3
Cooling Rate Variations Within the Textural Classes

Band Width (mm)	Class	Number of Meteorites	Ni Variation (wt%)	Cooling Rates Variation (°C/m.y.)
> 2 mm	Ogg	9	<7-7.5	0.8-6
1.0-2.0	Og	67	7.0-8.9	0.8-12
0.5-1.0	Om	51	7.0-12.0	0.4-25
0.25-0.5	Of	36	7.5-13.5	0.4-100
<0.25	Off	4	13.0-18.0	0.8-12
<0.25	Off-D	9	9.8-18.1	0.4-500
<0.25	D	17	12.4-30.0	0.8-500

Table 4
Resolved Ga-Ge-Ni Groups (Wasson, 1967a, b, c)

Group	Structure	Ni Variation (wt %)	Ge Variation (ppm)	Number of Members Studied	Variation in Cooling Rate (°C/m.y.)
I	Og-Ogg	<7.0-8.2	238->371	10	2-3
IIIa	Om-Og	7.5-8.7	33-47	26	1.5-10
IIIb	Om	9.0-10.7	28-38	14	1-2
IVa	Of	7.5-9.8	.092-.146	20	7-90
IVb	D	16.2-18.2	.03-.06	8	2-25

Table 5
Iron Meteorites in Group I

Meteorite	Band Width (mm)	Ni (±0.1 wt%)	Ge (±10ppm)	P (wt%)	Cooling Rate (°C/my)
Cranbourne	~ 2	7.0	371	---	3
Canyon Diablo					
Ashfork	2.5	7.0	331	---	2
#1	1.9	7.2	328	---	2.5
#2	1.3	8.1	319	0.34	2.5
#3	1.2	8.2	334	0.17	2.2
Bogou	1.8	7.1	301	---	3
Karee Kloof	~1.7	7.7	320	---	~2
Odessa	1.6	7.5	296	---	3
Bischtübe	1.5	8.0	238	---	2
Toluca	1.1	8.2	246	---	2

Table 6
Iron Meteorites in Group IIIa

Meteorite	Band Width (mm)	Ni (± 0.1 wt%)	Ge (± 1 ppm)	P (wt %)	Cooling Rate ($^{\circ}\text{C}/\text{m.y.}$)
Williamstown	0.85	7.5	33	.075	10
Costilla Peak	1.0	7.5	34	0.08	7
Nativitas (Santa Apolonia)	1.0	7.5	~ 35	---	7
Henbury	0.9	7.5	34	---	8
Norfolk	1.05	7.5	38	---	6
Cape York	1.55	7.6	36	0.14	3
Willamette	~ 1.0	7.6	37	---	6
Madoc	0.8	7.65	~ 36	---	10
Descubridora	1.15	7.7	~ 40	---	4
Sacramento Mtns.	1.0	7.7	37	---	5
Boxhole	0.8	7.7	37	---	8
San Angelo	0.85	7.7	39	0.10	7.5
Casas Grandes	1.05	7.8	~ 37	---	4
Canyon City	1.0	7.8	36	---	5
Merceditas	1.0	7.9	40	---	4.5
Norfork	0.9	7.9	41	0.14	5
Apoala (pseudo)	0.85	8.2	43	0.19	4
Providence	1.2	8.3	42	---	2
Drum Mountains	1.1	8.3	42	---	2
Franceville	1.0	8.3	42	---	3
Trenton	0.95	8.3	45	---	2.5
Carthage	1.2	8.4	44	---	2
Tamarugal	1.0	8.4	44	---	2
Aggie Creek	1.2	8.5	40	---	1.5
Spearman	1.0	8.7	46	---	2
Ruff's Mountain	1.1	8.7	47	---	1.5

Table 7
Iron Meteorites in Group IIIb

Meteorite	Band Width (mm)	Ni (± 0.1 wt%)	Ge (± 1 ppm)	P (wt%)	Cooling Rate ($^{\circ}\text{C}/\text{m.y.}$)
Cleveland	1.05	8.9	41	---	1.5
Mount Edith	0.75	9.1	38	---	2
Grant	0.8	9.3	38	---	1.5
Ereece	0.85	9.4	38	---	1.2
Sanderson	0.75	9.4	36	---	1.2
Roper River	0.75	9.8	34	---	1.2
Verkhne Dnieprovsk	0.75	9.9	33	---	1.2
Sams Valley	0.8	9.9	35	---	1.0
Bear Creek	0.75	10.0	33	0.62	1.2
Bella Roca	0.75	10.1	31	0.21	$1.5 \pm .5$
Tambo Quemado	0.75	10.1	31	----	1.2
Cuernavaca	0.6	10.4	32	---	1.3
Chupaderos	0.6	10.4	31	---	1.2
Tieraco Creek	0.5	10.7	28	---	1.5

Table 8
Iron Meteorites in Group IVa

Meteorite	Band Width (mm)	Ni (± 0.1 wt%)	Ge (± 0.013 ppm)	P (wt%)	Cooling Rate ($^{\circ}\text{C}/\text{m.y.}$)
Yanhuítlan	0.35	7.5	0.103	---	80
Jamestown	0.30	7.5	0.093	---	90
Social Circle	0.35	7.5	0.092	---	70
Western Arkansas	0.35	7.7	0.10	---	65
Maria Elena	0.3	7.7	0.096	---	70
La Grange	0.33	7.7	0.120	---	70
Huizopa	0.3	7.8	0.122	---	65
Bishop Canyon	0.3	7.9	0.116	---	65
Putnam County	0.3	7.9	0.130	---	60
Gibeon	0.35	8.0	0.111	---	50
Charlotte	0.40	8.1	0.116	---	18
Para de Minas	0.38	8.1	0.125	0.06	25
Bristol	0.30	8.2	0.125	---	50
Seneca Township	0.45	8.5	0.124	---	12
Altonah	0.35	8.6	0.123	---	18
Bugaldi	0.40	9.0	0.135	---	10
Hill City	0.37	9.3	0.146	---	10
New Westville	0.40	9.4	0.139	---	7
Duchesne	0.25	9.5	0.126	---	12
Chinaulta	0.35	9.5	0.113	---	8

Table 9
Iron Meteorites in Group IVb

Meteorite	Band Width (mm)	Ni (wt%)	Ge (ppm)	Cooling Rate (°C/m.y.)
Tlacotepec	~ 0.03	~ 16.2	~ .03	~ 8
Kokomo	~0.06	~ 16.2	~.03	~ 2
Hoba	~ 0.03	~ 16.2	~ .03	~ 9
Cape of Good Hope	~ 0.03	16.3	~ .04	~ 7
Chinga	~ 0.015	16.5	< 0.18	~ 25
Weaver Mountains	~ 0.01	18.0	~ 0.05	~ 20
Klondike	~ 0.01	~ 18.2	~ 0.05	~ 20
Tawallah Valley	~ 0.01	18.2	~ 0.06	~ 20

Table 10
Carbon Contents of Iron Meteorites
(Moore and Lewis, 1967)

Meteorite	Group	C (wt %)	P (wt %)	Ni (wt %)
Canyon Diablo (plain)	I	0.11	-	7.2
Canyon Diablo (rim)	I	0.33	-	7.2
Orange River	Possible IIIa & IIIb	0.01	0.25	8.6
Casimiro de Abreu	"	0.009	0.24	8.5
Costilla Peak	IIIa	0.04	0.08	7.5
Kenton County	Possible IIIa	0.005	0.08	7.5
Para' de Minas	IVa	0.01	0.06	8.2
Yanhuitlan(Misteca)	"	0.003	-	7.5

Table 11
Summary of Correlations of Various Parameters with Respect to Increasing Ni Content
within the Ga-Ge Groups

As Ni Content Increases						
Group	Ge	Cooling Rate	Exposure Age	Bandwidth	Plessite	Inclusion Content
I	Decreases	No Change	Variable	Decreases	α in Widmanstätten Pattern	Large-Constant
IIIa	Increases	Decreases	Constant $600-700 \times 10^6$ yrs	No Change	Rounded Taenite Decomposed	Small-Increasing
IIIb	Decreases	No Change	Constant $600-700 \times 10^6$ yrs	Decreases	α in Widmanstätten Pattern α_2 in Widmanstätten Pattern	Large-Constant
IVa	Decreases	No Change	Constant 400×10^6 yrs	No Change	Rounded Taenite Decomposed	Small-Increasing
IVb	Increases	Increases (?)	Variable	Decreases	Ataxite	Very Small Increasing

Table 12
Meteorites Which Are Not Members of Ga-Ge Groups

Outside Ga-Ge-Ni Correlations

Meteorite	Ni (wt%)	Ge (ppm)	Bandwidth (mm)	Class	Cooling Rate (°C/m.y.)
Nelson County	6.9	0.84(W)	5	Ogg	0.8
Clark County	7.0	0.98(W) 0.65(S)	1.2	Og	8
Bagdad	7.8	100(S)	1.1	Og	5
Goose Lake	8.3	305(W) 290(S)	1.2	Og	2
Kingston	7.0	55(S)	0.9	Om	12
Moonbi	8.0	0.82(S)	0.55	Om	12
Hammond Township	8.2	58(W)	0.7	Om	7
Gun Creek	8.5	70(W)	0.75	Om	4
Richa	8.7	72(H)	0.95	Om	2
Mbosi	8.9	27(W)	0.8	Om	2
Knowles	9.1	31(W)	0.9	Om	1.5
Grand Rapids	9.4	14(W) 15(S)	0.55	Om	3
Mertzon	9.6	295(W)	0.9	Om	1.0
Delegate	9.5	42(W)	0.8	Om	1.2
Thurlow	9.9	28(W)	0.8	Om	1.0
Cambria	10.3	1.6(W)	0.65	Om	1.5
Carbo	10.0	87(W)	0.8	Om	1.0
Rodeo	10.0	95(W)	0.55	Om	2
Brenham	11.1	72(W)	0.95	Om-P	0.4
Glorieta	11.8	11(W)	0.85	Om-P	0.4
St. Genevieve	8.0	0.8(W)	0.45	Of	20
Hualapai	11.6	102(W)	0.4	Of	1.0
Victoria West	11.7	31(W)	0.35	Of	1.2
Edmonton (Kentucky)	12.7	35(W)	0.28	Of	1.0
Carlton	12.8	8.7(W)	0.15	Off	3
Tazewell	16.7	4.0(W)	0.05	Off	2

Table 12 (Continued)
Meteorites Which Are Not Members of Ga-Ge Groups

Outside Ga-Ge-Ni Correlations

Meteorite	Ni (wt%)	Ge (ppm)	Bandwidth (mm)	Class	Cooling Rate (°C/m.y.)
Perryville	9.8	77(L)	~0.08	Off-D	~250
Ballinoo	9.8	91(W) 100(S)	~0.08	Off-D	~200
Bacubirito	9.8	29(W)	~0.07	Off-D	~200
Arltunga	10.1	68(L)	~0.005	Off-D	~500
Monahans	10.9	127(W)	~0.025	Off-D	~500
Wiley	11.8	114(W)	~0.05	Off-D	~65
Mt. Magnet	14.7	5.3(W)	0.02	Off-D	50
Butler	16.0	2000(W)	0.15	Off-D	0.4
Dayton	18.1	3.5(W)	~0.035	Off-D	~2
Illinois Gultch	12.4	2.9(S)	~0.05	D	~40
Deep Springs	13.4	0.108(W)	~0.01	D	~400
Cowra	13.0	12(W)	~0.075	D	~7
Piñon	16.6	1.2(W)	~0.02	D	~12
Shingle Springs	17.0	0.13(W)	~0.01	D	~50
S. Byron	18.2	45(W)	~0.01	D	~20
Morradal	~18.8	119(W)	~0.01	D	~15

Table 12 (Continued)
 Meteorites Which Are Not Members of Ga-Ge Groups

Outside Cooling Rate – Bandwidth – Ni Correlations

Meteorite	Ni (wt%)	Bandwidth (mm)	Class	Cooling Rate (°C/m.y.)
Chihuahua City	6.9	~7	Ogg	< 1
Cruz del Aire	9.2	0.65	Om	3
Abancay	7.9	0.55	Om	15
Elbogen	10.3	~0.8	Om	0.8
Red River	9.8	0.92	Om	0.8
Arlington	8.6	0.5	Om	8
Woodbine	12.6	0.3	Of	1.0
Pitts	13.0	0.27	Of	0.8
Laurens County	13.4	0.35	Of	0.5
Persimmon Creek	13.6	0.06	Off	10
Follinge	18.0	0.04	Off	1.5
Iquique	16.0	~0.01	D	80
Twin City	16.0	~0.001	D	~0.8

References

- (W) Wasson (1966, 1967a, b, c)
- (S) Smales (1967)
- (L) Lovering (1957)
- (H) Hey (1967)

Table 13
Possible Members of Group I

Meteorite	Bandwidth (mm)	Ni (wt%)	Ge (ppm)	P (wt%)	Cooling Rate (°C/m.y.)
Arispe	2.3	6.6-7.0	229 (Smales, 1967)	—	> 2
Mooranoppin	~ 2	6.9	396 (Lovering, 1957)	—	~3.5
Youndegin	2.5	6.9	312 (Smales, 1967)	—	2
			322 (Lovering, 1957)		
Mt. Stirling	2.4	6.9	409 (Lovering, 1957)	—	3
Yenberrie	1.9	7.0	344 (Lovering, 1957)	—	3
Rifle	1.9	7.3	—	0.15	2
Bohumilitz	1.9	7.3	273 (Smales, 1967)	—	2
Bahjoi	1.3	7.4	—	—	3.5
Lexington County	2.0	7.45	—	—	2
Annaheim	1.5	7.5	—	—	3
Samelia	1.2	8.0	—	—	3
Ogallala	1.7	8.1	—	—	1
Briggsdale	1.2	8.3	—	0.18	2
Deport	1.5	8.4	—	—	1
Mazapil	1.0	8.4	—	—	2.5

Table 14
Possible Members of Group IIIa

Meteorite	Bandwidth (mm)	Ni (wt%)	Ge (ppm)	P (wt%)	Cooling Rate (°C/m.y.)
Basedow Range	1.0	7.4	30 (Lovering, 1957)	—	7
Kenton County	0.85	7.5	—	0.08	8
Livingston	1.0	7.5	—	—	7
Cacaria	1.0	7.7	—	—	6
Canton	1.0	7.7	39 (Smales, 1967)	—	5
Morito	1.0	7.7	—	—	7
Tonganoxie	1.25	7.8	—	0.12	3.5
Loreto	1.2	7.8	—	0.15	3.5
Billings	1.3	7.9	38 (Smales, 1967)	0.10	3
Chilkoot	1.0	7.9	—	—	4
Harriman	0.95	7.9	—	—	5
Bear Lodge	1.1	7.9	—	0.14	4
Roebourne	1.25	8.0	49 (Lovering, 1957)	—	2.5
Leeds	1.2	8.1	—	—	2
Cumpas	1.15	8.1	—	—	2.2
Puente del Zacate	1.0	8.2	—	—	3
Charcas	0.9	8.2	—	0.13	4
Thunda	1.6	8.3	39 (Lovering, 1957)	—	1.2
Kyancutta	1.14	8.3	42 (Lovering, 1957)	—	2
Gundaring	0.8	8.3	38 (Lovering, 1957)	—	4
Coopertown	1.5	8.5	32 (Lovering, 1957)	0.19	1.2

Table 15
Possible Members of Group IIIb

Meteorites	Band Width (mm)	Ni (wt %)	Ge (ppm)	P (wt %)	Cooling Rate (°C/m.y.)
Treysa	0.95	8.9	43 (Wasson, 1967c)	---	1.5
Wonyulgunna	0.8	9.05	34 (Lovering, 1957)	---	2
Joe Wright Mtn.	0.95	9.2	---	0.46	1.5
Concepcion	0.6	10.0	---	0.48	1.5
Narraburra	0.5	10.2	29 (Lovering, 1957)	---	2
Mungindi	0.3	11.2	22 (Wasson, 1967c)	---	2
Anoka	0.33	11.8	16.2 (Wasson, 1967c)	---	1.5

Table 16
Possible Members of Group IIIa-IIIb

Meteorite	Band Width (mm)	Ni (wt %)	Ge (ppm)	P (wt %)	Cooling Rate (°C/m.y.)
Casimiro de Abreu	1.3	8.5	---	0.24	1.5
Campbellsville	1.25	8.6	45 (Smales, 1967)	0.27	1.0
Orange River	1.5	8.6	---	0.25	1.0
Lenarto	1.3	8.7	---	0.25	1.0
Owens Valley	1.15	8.7	---	0.20	2
Plymouth	1.05	8.7	---	0.24	2
Staunton	1.45	8.8	---	0.24	1.0
Willow Creek	1.4	8.8	---	---	1.0
El Capitan	1.0	8.8	---	---	1.8
Bartlett	1.1	8.9	---	---	1.5

Table 17
Possible Members of Group IVa

Meteorite	Band Widths (mm)	Ni (wt %)	Ge (ppm)	P (wt %)	Cooling Rate (°C/m.y.)
Obernkirchen	0.25	7.7	0.2 (Smales, 1967)	---	100
Chile	0.35	7.7	---	0.02	70
Nejed	0.3	7.8	---	0.03	70
Otchinjau	0.35	8.0	< 1 (Hey, 1967)	---	50
Bodaibo	0.3	8.05	---	---	60
Mart	0.4	9.3	---	0.13	7
Duel Hill (1854)	0.42	10.2	---	0.15	3

Table 18
Members and Non-Members of
Ga-Ge Groups (Summary)

Textural Group	Number of Meteorites Studied in Each Textural Group	% of Meteorites which are Members of Ga-Ge Groups	Number of Meteorites not in Ga-Ge Groups
Ogg, > 2mm	9	77	2
Og, 1-2mm	67	95	3
Om, 0.5-1mm	51	65	18
Of, 0.25-0.5	36	81	7
Off, < 0.25	4	0	4
Off-D < 0.25	9	0	9
D < 0.25	<u>17</u>	<u>47</u>	<u>8</u>
	Sum 193	Average 71%	Sum 55

Ni-Fe PHASE DIAGRAM (GOLDSTEIN & OGILVIE, 1965A)

TEMPERATURE, °C

γ TAENITE

α + γ

M_S

α

KAMACITE

□ HEXAHEDRITES (H)

□ COARSE OCTAHEDRITES (Op)

□ MEDIUM OCTAHEDRITES (Om)

□ FINE OCTAHEDRITES (Of)

ATAXITES (D)

TRANSITIONAL

PLESSITIC

TAENITIC

□ PALLASITES (P)

WT. % Ni

50

40

30

20

10

5

0

900

800

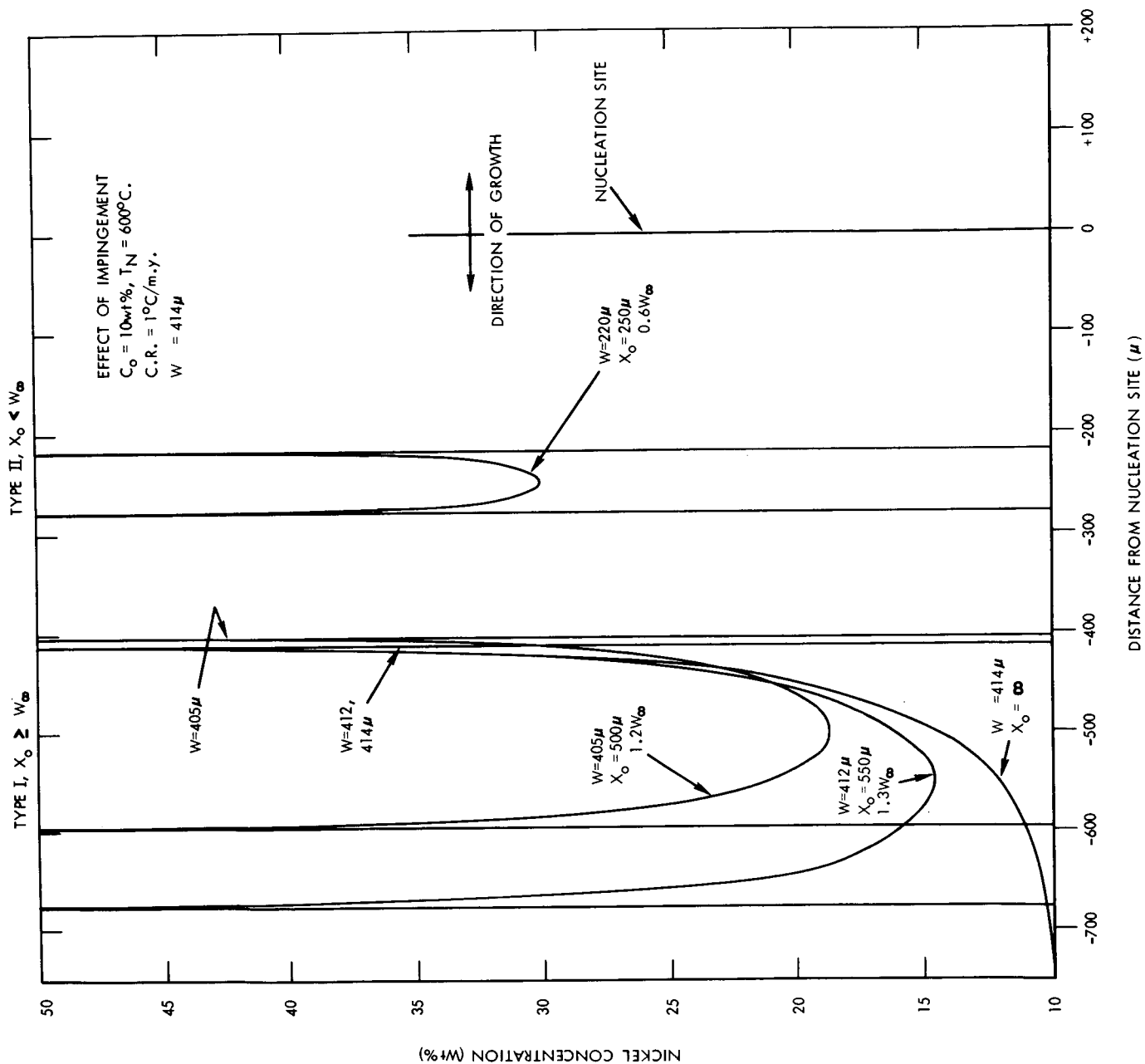
700

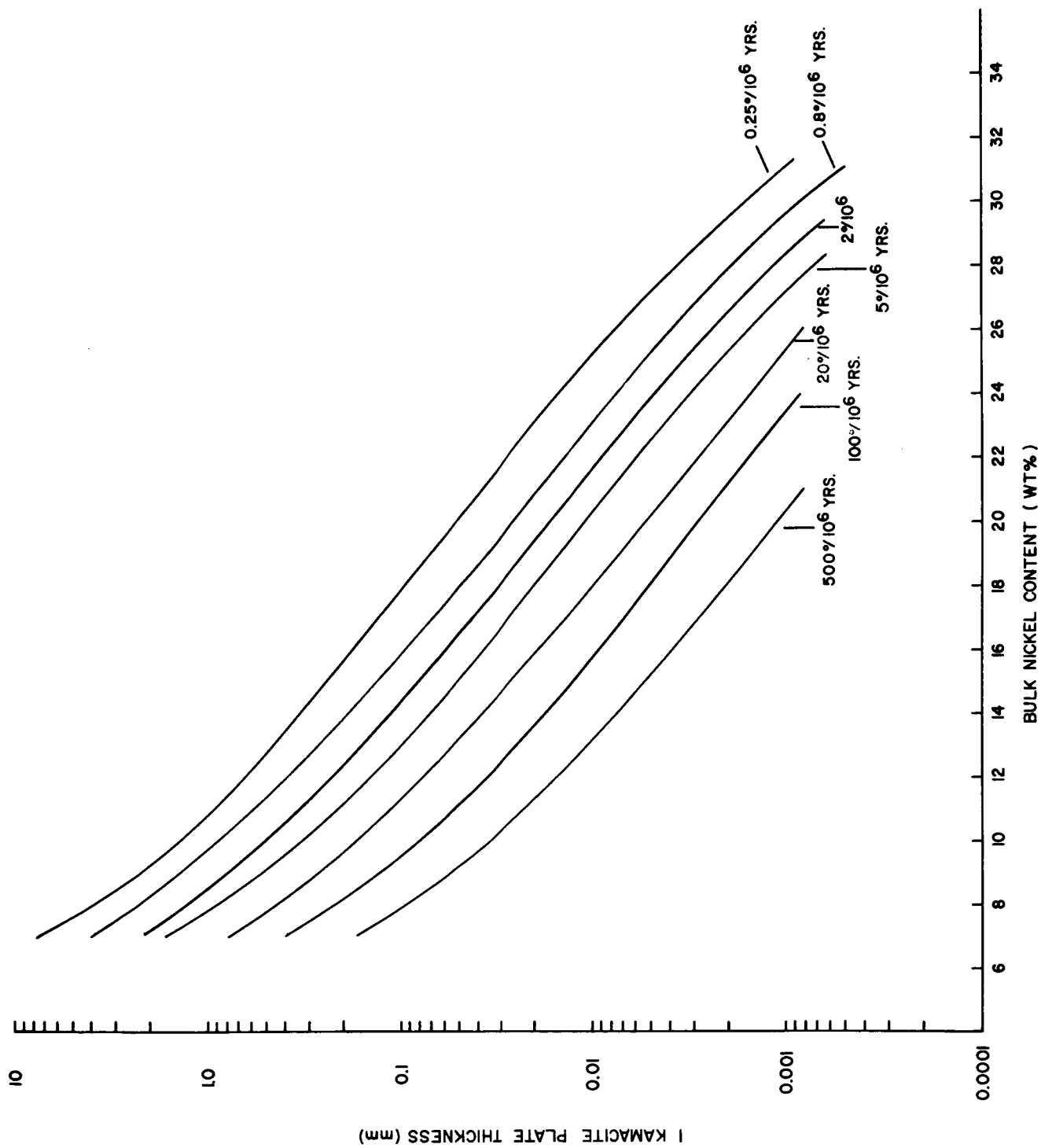
600

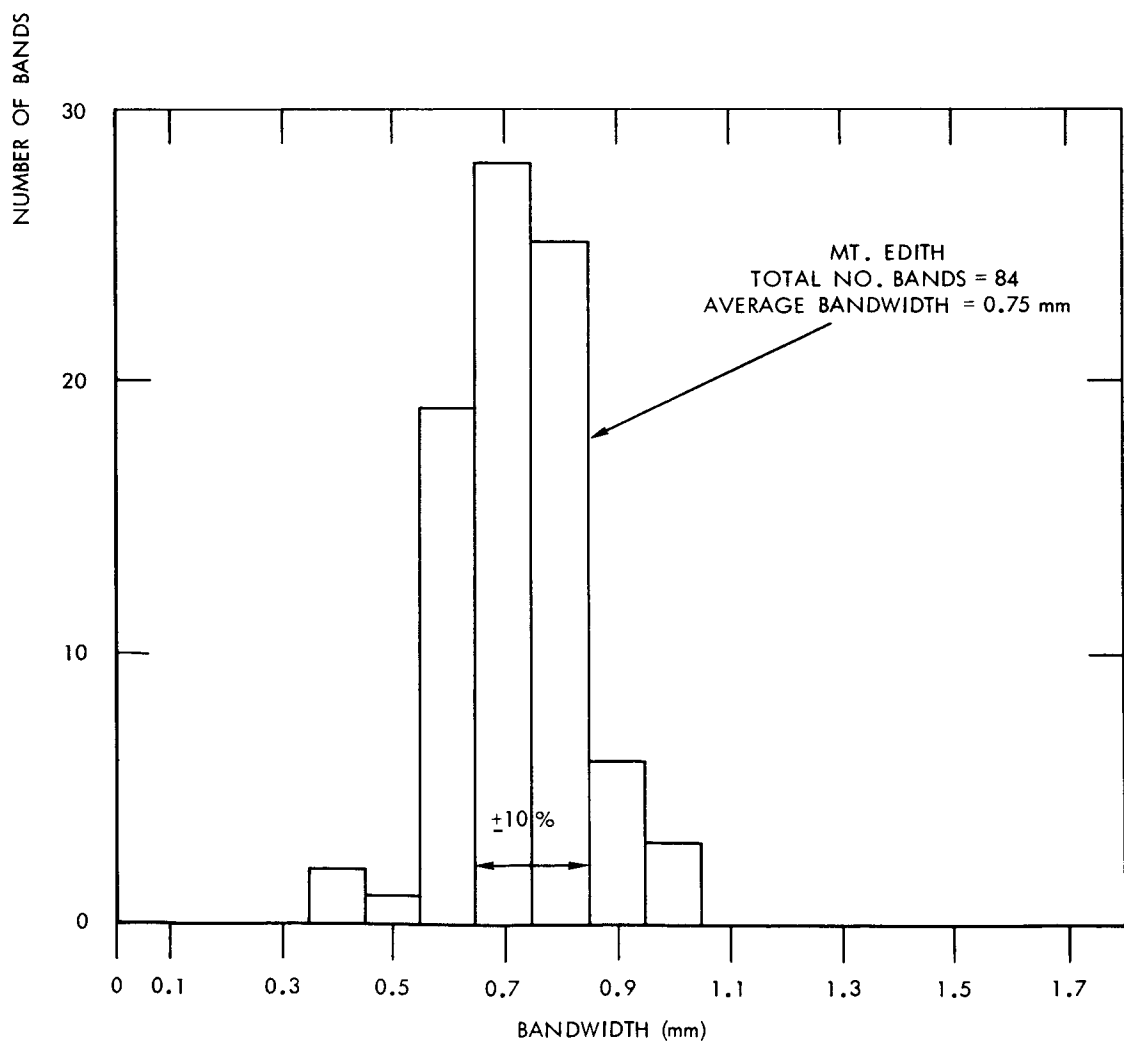
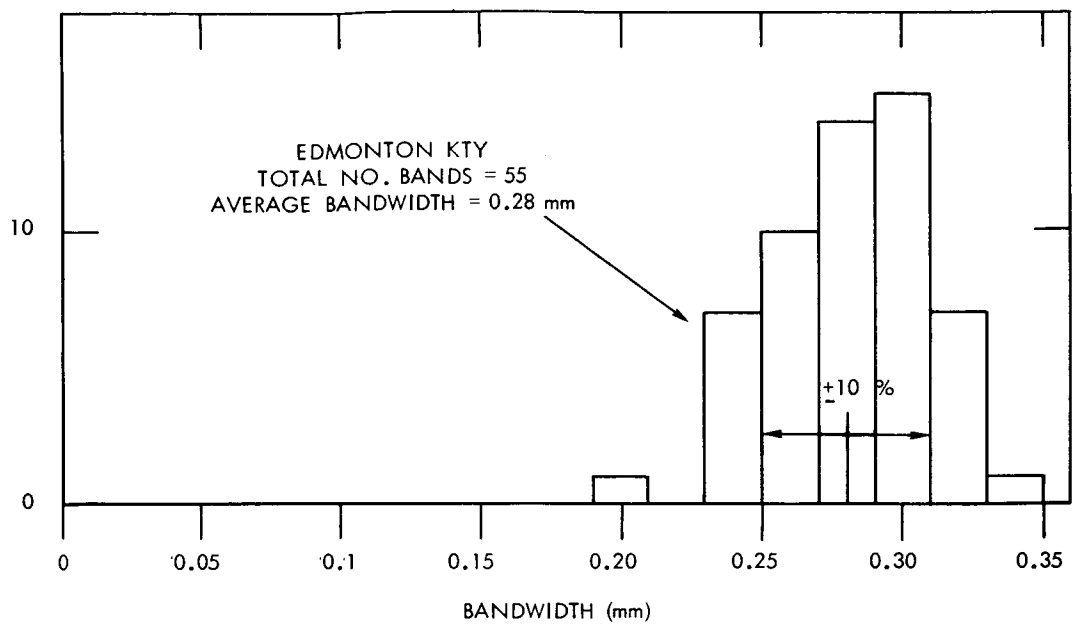
500

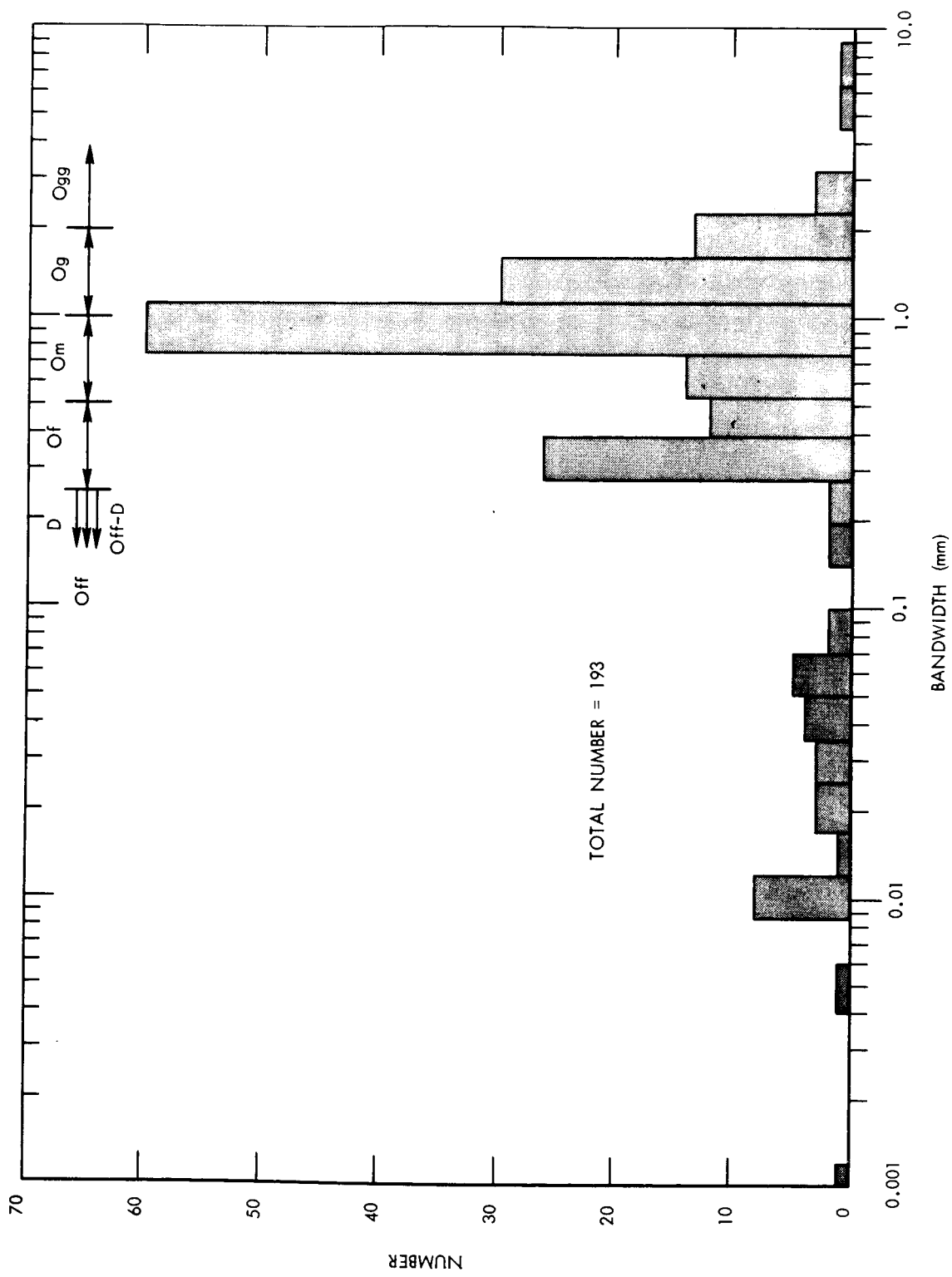
400

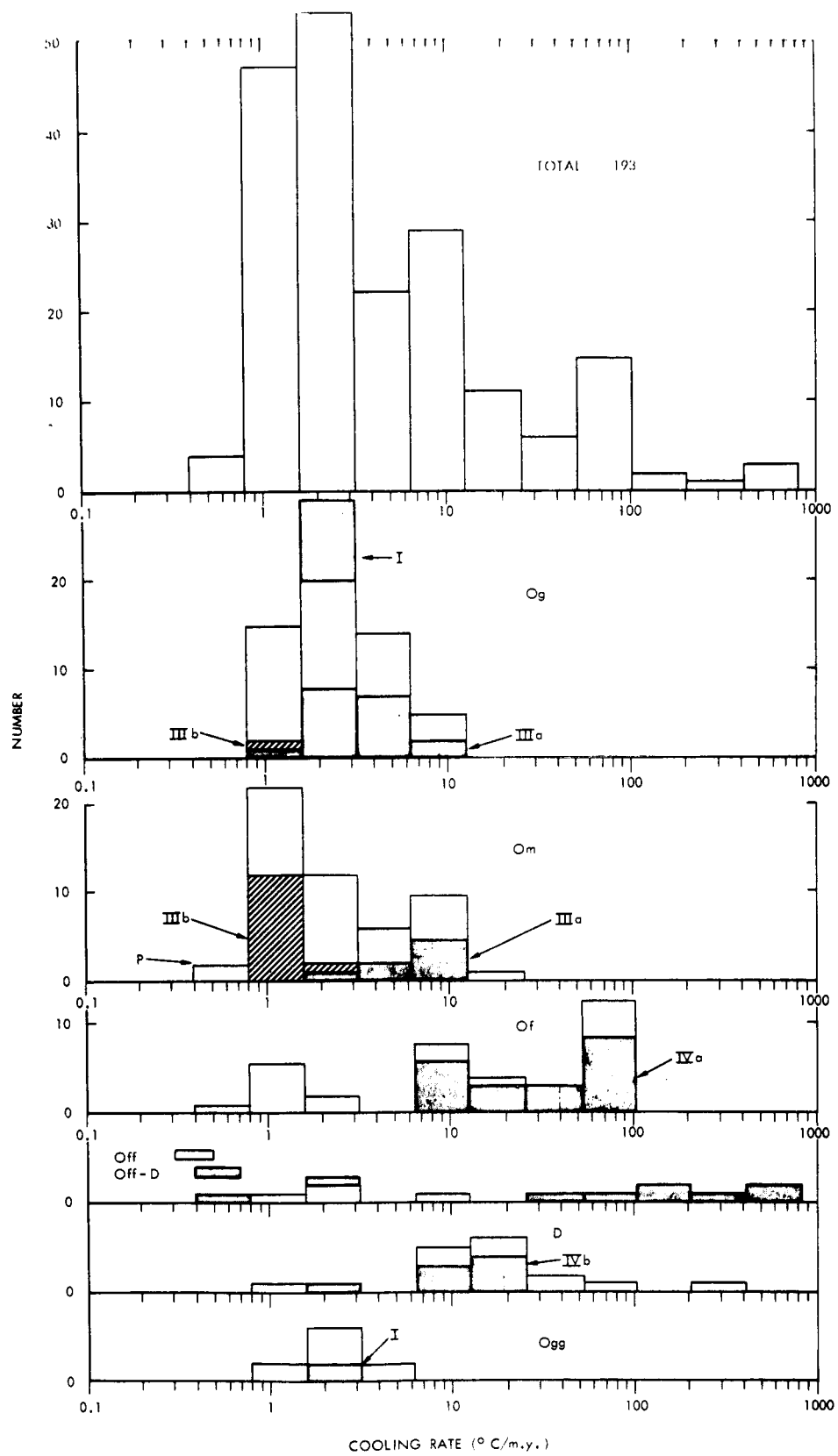
300

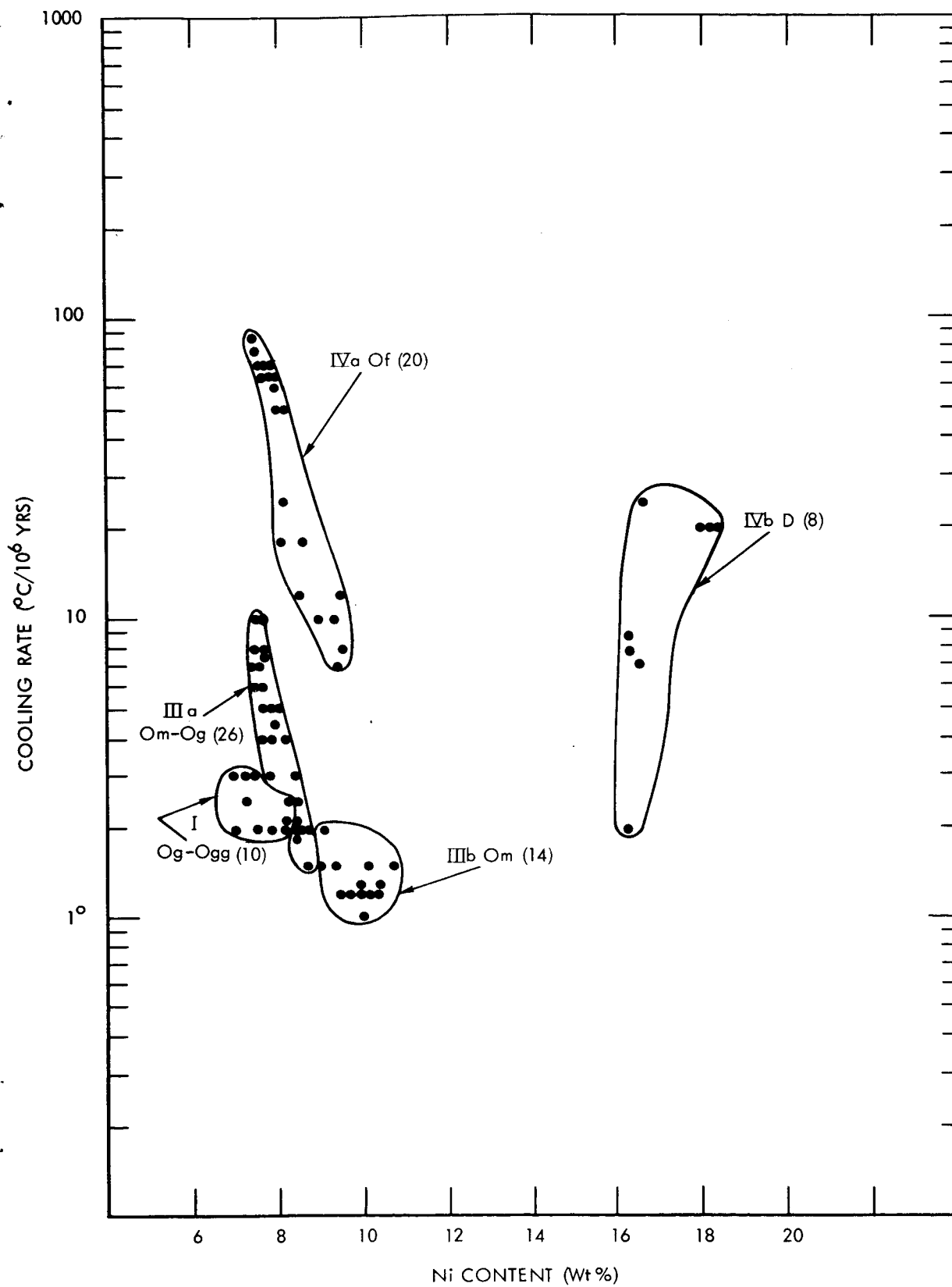


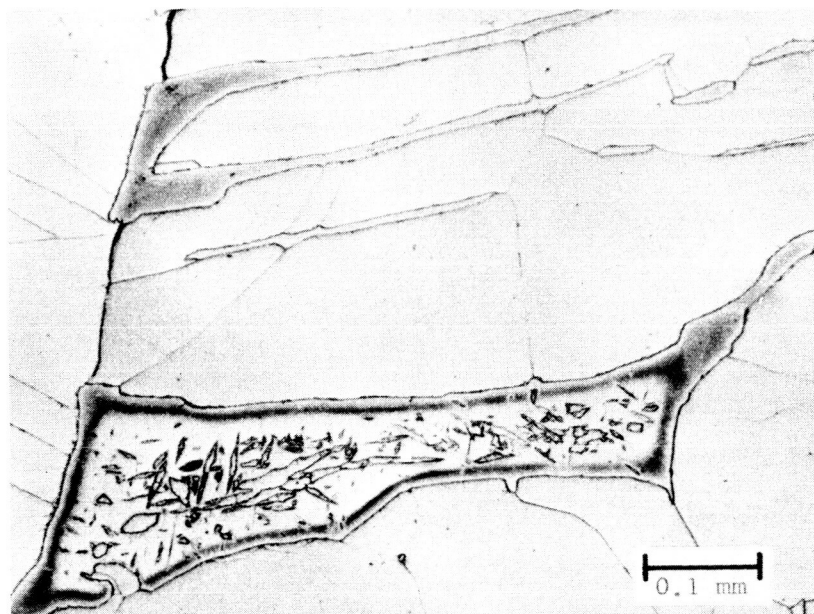




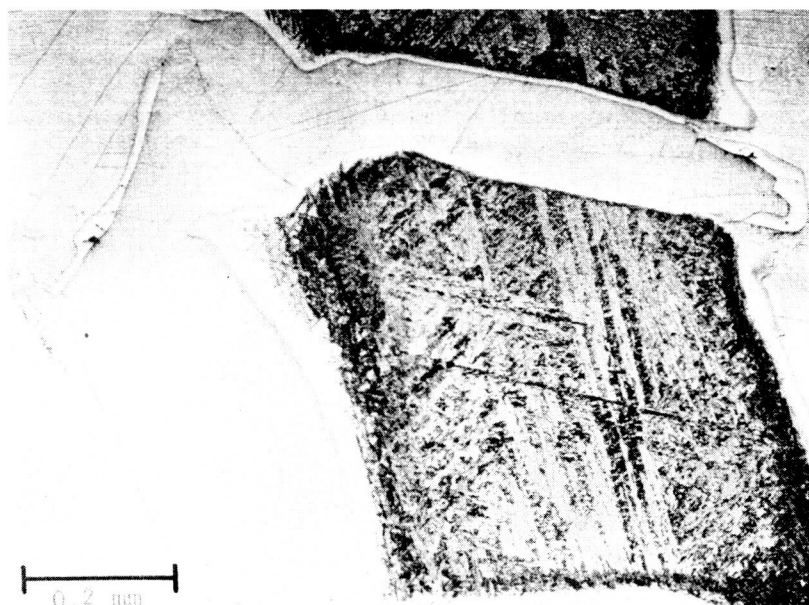




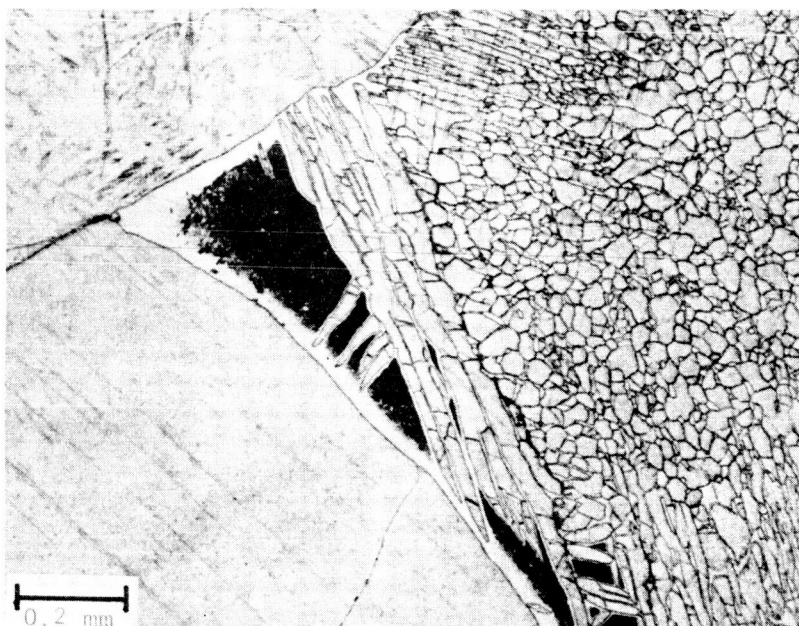




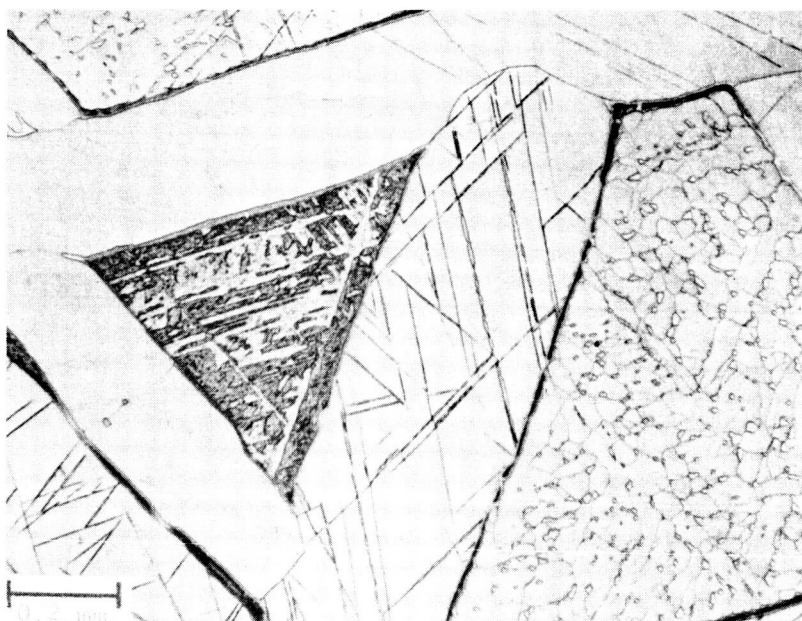
TOLUCA, GROUP I, COOLING RATE $2^{\circ}\text{C}/\text{my}$,
 8.1 wt.% Ni
 ETCHANT 1% NITAL.



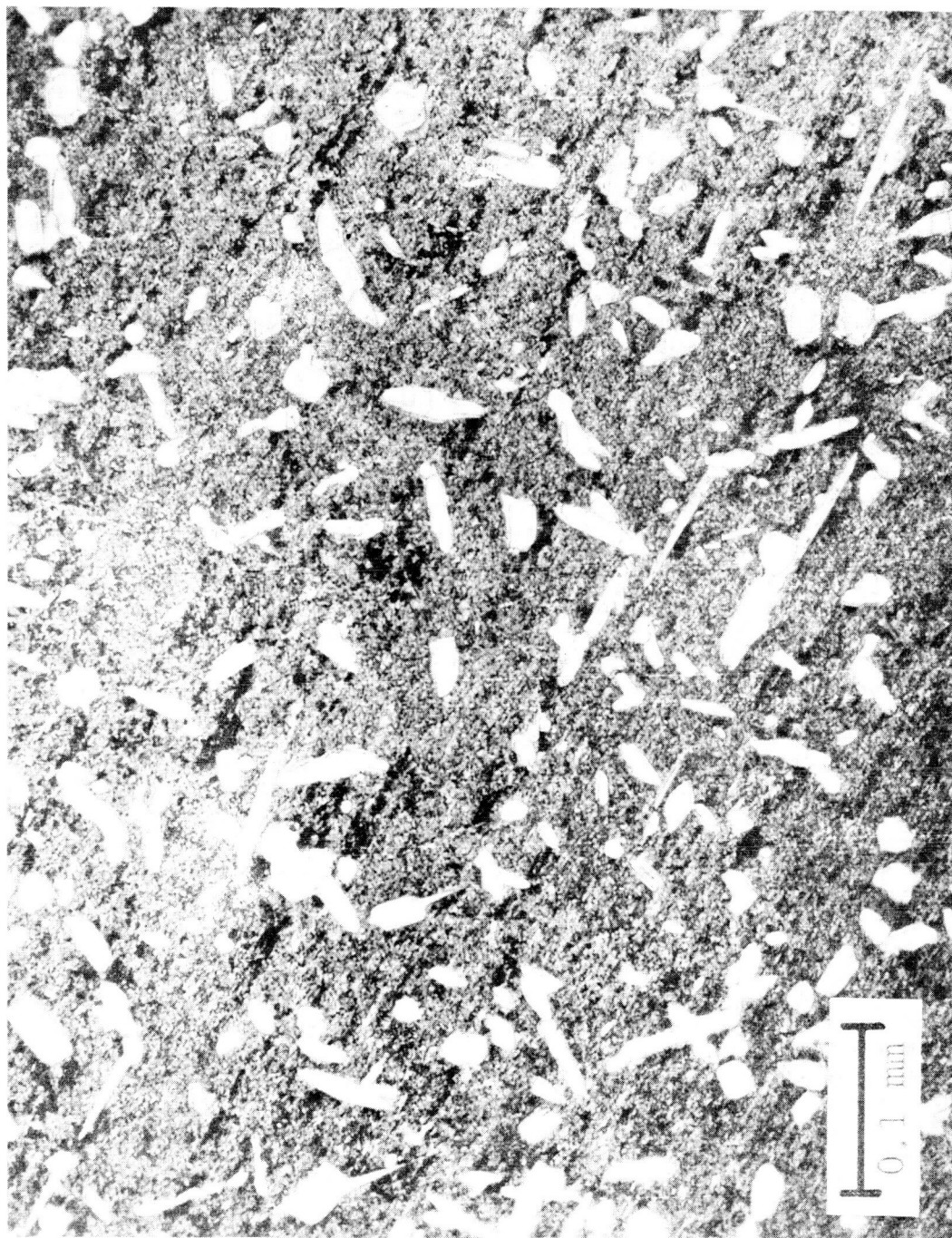
GRANT, GROUP IIIb, COOLING RATE $1.5^{\circ}\text{C}/\text{my}$,
 9.6 wt.% Ni
 ETCHANT 1% NITAL.



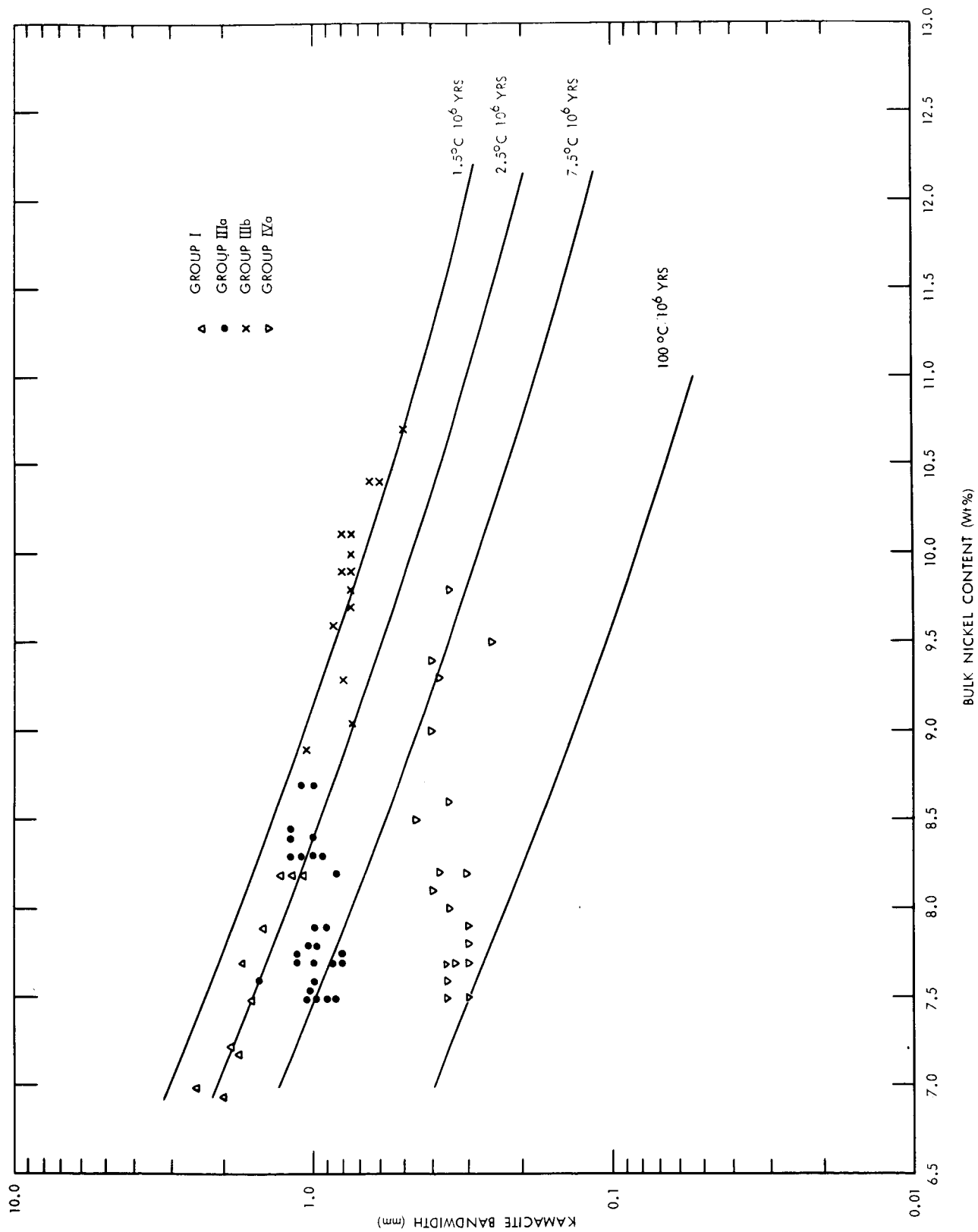
SPEARMAN, GROUP IIIa, COOLING RATE $2^{\circ}\text{C}/\text{my}$,
 8.7 wt. % Ni
 ETCHANT 1% NITAL.



BRISTOL, GROUP IVa, COOLING RATE $50^{\circ}\text{C}/\text{my}$,
 8.2 wt. % Ni
 ETCHANT 1% NITAL.



WEAVER MOUNTAINS, GROUP IVb,
COOLING RATE $20^{\circ}\text{C}/\text{my}$, 18.0 wt.% Ni
ETCHANT 1% NITAL.



COOLING RATE FOR DIFFERENT SIZED METEORITE PARENT BODIES

